epigenomes

MDPI

Article

DNA Methylation Suppression by *Bhendi Yellow Vein Mosaic Virus*

Kandhalu Sagadevan Dinesh Babu [1], Ashirbad Guria [1], Jeyalakshmi Karanthamalai [1], Nagesh Srikakulam [1], Kamlesh Kumari [1,2], Priyanka Sharma [1,3], Sam Aldrin Chandran [1,4], Anburaj Daniel Barnabas [5], Jebasingh Tennyson [6] and Gopal Pandi [1,*]

1 Department of Plant Biotechnology, School of Biotechnology, Madurai Kamaraj University, Madurai 625021, India; ksdineshbabumku@gmail.com (K.S.D.B.); ashir.biotech@gmail.com (A.G.); jeyasweety92@gmail.com (J.K.); bioinagesh@gmail.com (N.S.); kamlesh.kumari407@gmail.com (K.K.); prnksharma862@gmail.com (P.S.); aldrin84@gmail.com (S.A.C.)
2 Department of Plant Molecular Biology, University of Delhi, South Campus, New Delhi 110021, India
3 Department of Genetic Engineering, School of Biotechnology, Madurai Kamaraj University, Madurai 625021, India
4 School of Chemical and Biotechnology, SASTRA University, Thanjavur 613401, India
5 Department of Botany, The American College, Madurai 625002, India; adbarnabas@gmail.com
6 Department of Plant Sciences, School of Biological Sciences, Madurai Kamaraj University, Madurai 625021, India; jebasinghs@gmail.com
* Correspondence: pgopal.biotech@mkuniversity.org; Tel.: +91-452-2458230

Received: 3 May 2018; Accepted: 29 May 2018; Published: 31 May 2018

Abstract: *Bhendi yellow vein mosaic virus* (BYVMV) belongs to the monopartite begomovirus associated with the β satellite. As a single-stranded DNA (ssDNA) virus, it should be amenable to transcriptional and post-transcriptional gene silencing (TGS and PTGS). Previously, we had demonstrated C2, C4 and βC1 to be having different levels of influence on PTGS. Hence in the present study, a series of experiments such as agroinfiltration, chop-polymerase chain reaction (PCR), quantitative PCR (qPCR) and bisulfite next generation sequencing (NGS) were designed to analyse the involvement of BYVMV proteins on DNA methylation suppression. From the preliminary studies, we concluded that BYVMV genes were responsible for TGS suppression and C2, C4 genes from BYVMV were selected for further studies. Agroinfiltration experiments with mutant C2 and C4 partial tandem repeat (PTR) constructs of BYVMV have confirmed the role of C2 and C4 in DNA methylation impairment. The protoplast replication assay has shown that C4 was not an impediment for viral DNA replication and subsequent agroinfiltration studies with the C4 mutant BYVMV PTR construct have revealed the involvement of C4 in viral DNA movement.

Keywords: begomovirus; DNA methylation; transcriptional gene silencing; suppressors; movement protein; *bhendi yellow vein mosaic virus*; bisulfite sequencing; next generation sequencing

1. Introduction

Geminiviruses are circular single-stranded DNA (ssDNA) viruses with twinned icosahedral particles that infect economically important plants and cause devastating effects on crop yield. Based on the genome organization, host range and vector, recently geminiviruses has been classified into nine genera *Becurtovirus*, *Curtovirus*, *Grablovirus*, *Mastrevirus*, *Turncurtovirus*, *Topocuvirus*, *Capulavirus*, *Eragrovirus* and *Begomovirus* [1]. Among these, the whitefly (*Bemisia tabasi*) transmitted begomovirus that infects dicot plants, is a diverse genus comprising of more than 288 species with either monopartite or bipartite genome [2]. Begomoviruses depend entirely on the host cellular machinery for their DNA replication, transcription, and translation [3,4]. They replicate via rolling circle replication (RCR) that

happens through the formation of the double-stranded DNA replicative form (RF). The intermediate RF is converted into a minichromosome using host proteins, which then serves as a template for viral DNA replication and bicistronic transcription [5].

RNA silencing of invaded viruses is mediated by the host small interfering RNAs (siRNAs) at post-transcriptional level [3,6] or at the chromatin level by histone/DNA modifications known as transcriptional gene silencing (TGS). Geminivirus minichromosomes succumb to TGS at chromatin level, either by the epigenetic modification of histone or by the methylation of DNA [7]. The addition of the methyl group to cytosine residues in the viral promoter is a stable modification that hinders viral DNA replication and transcription [8,9]. The pattern of DNA methylation is conserved across the plant kingdom which is constantly maintained by the domain rearranged DNA methyltransferases (DRM1), methyltransferases 1 (MET1) and Chromomethylases [10–12]; these enzymes methylate CG, CHG and CHH sites, respectively. DNA methylation on promoter sequences prevents active gene transcription [13,14]. It has been established that AC1, AC2/C2 and V2 of begomovirus and βC1 of β satellite have the capacity to interfere with the DNA methylation cycle by affecting the methylation pathway proteins either directly or indirectly. These results suggest the suppression of methylation-mediated gene silencing by begomoviral proteins [15–18].

Bhendi yellow vein mosaic virus (BYVMV) is a monopartite begomovirus, associated with a β satellite molecule (Figure 1E,F). BYVMV is needed for DNA replication, encapsidation and viral movement, while β satellite is essential for high accumulation of viral DNA and the expression of typical symptoms [19,20]. Apart from the βC1, BYVMV C2 and C4 also have a varying degree of post-transcriptional gene silencing (PTGS) suppressor activity [21,22]. Mutation on BYVMV C2 drastically reduces viral DNA accumulation, which hints at a possible role of C2 in viral DNA replication [23]. To understand the suppression of TGS by BYVMV, the present work has been carried out.Analyses of C4 and C2 mutations by the high depth bisulfite next generation sequencing (NGS) revealed that both genes interfere with the DNA methylation. Intriguingly, plants co-infiltrated the with partial tandem repeat construct of C4 mutant BYVMV (C4MAPTR, refer Section 4.1) and βPTR (GenBank ID: AJ308425.1) remained asymptomatic. Further, studies on the protoplast and emerging leaf revealed that C4 has been involved in virus movement.

2. Results

2.1. BYVMV Interferes with DNA Methylation

It is well known that BYVMV is having C2, C4 and βC1 as suppressors with varying degrees of PTGS suppression [22]. C4 and βC1 are also symptom determinants [24–27]. To understand BYVMV interference in the TGS pathway, we infiltrated pCAMBIAAPTR9 along with pBINβPTR4 (hereafter referred to as APTR and βPTR) (GenBank ID: AF241479.1 and AJ308425.1) into *N. benthamiana* plants and the infiltrated plants showed severe leaf curling at 21 days of post-infiltration (dpi). Polymerase Chain Reaction (PCR) screened plants were subjected to qPCR (Quantitative PCR) and Southern hybridization to assure the BYVMV high accumulation as we demonstrated previously (Figure 1) [22,23]. The viral DNA isolated from 13 *N. benthamiana* plants co-infiltrated with APTR and βPTR was digested with MSREs (Methylation-Sensitive Restriction Enzymes) such as *Sau3AI*, *MboI* and *HpaII* for chop-PCR. The MSRE's digested viral DNA sample was used for chop-PCR using primers of intergenic region (IR) (Table 1, Primers 1 and 2), V2 (Table 1, Primers 3 and 4), C2 (Table 1, Primers 5 and 6), C4 (Table 1, Primers 7 and 8), βC1 (Table 1, Primers 9 and 10) and its upstream region (Table 1, Primers 11 and 12). The result showed a prominent reduction in amplification at least in one among the three enzymes (Supplementary Figure S1) when compared to undigested product. Intriguingly, complete reduction was observed with the C4 forward and V2 reverse primers which lie between the C4 and V2 genes yielding a 1.1 kb product (Supplementary Figure S1B). To substantiate chop-PCR results, we performed qPCR to precisely estimate the copy number on digested viral DNA using BYVMV or a β satellite-specific primer and found over 90% reduction in *HpaII* or *MboI* digestion,

respectively. In addition, the other two enzymes also showed >50% reduction of amplification when quantified using BYVMV or β satellite-specific primers, suggesting most of the viral DNA remains unmethylated (Figure 2A,B). In chop-PCR and subsequent qPCR, we observed an amplification of viral DNA sequences with the MSRE digested samples. This is because the efficiency of chop-PCR depends on the availability of an MSRE site within the amplicon, enzyme activity and the presence of methylated DNA, which is mediated by the initial response of *N. benthamiana*. Chop-PCR and qPCR roughly reveal that BYVMV is impairing the DNA methylation.

In order to examine the methylation level of the viral DNA precisely and accurately, we preferred the bisulfite method followed by the NGS (next generation sequencing). Though there are different methods available for DNA methylation analysis, bisulfite sequencing is considered as a "gold standard" for single base resolution measurement of DNA methylation. Bisulfite coupled with the NGS method gives greater advantages over the conventional method of methylation analysis. DNA methylation analysis by conventional bisulfite conversion, cloning and sequencing of an individual clone is a long, time-consuming process whereby interpretation of the DNA methylation level is carried out by analysing 10 to 20 clones corresponding to the specific genomic loci. In contrast to this, the bisulfite-NGS method gives the greater advantage of analysing methylation levels at whole genome level.

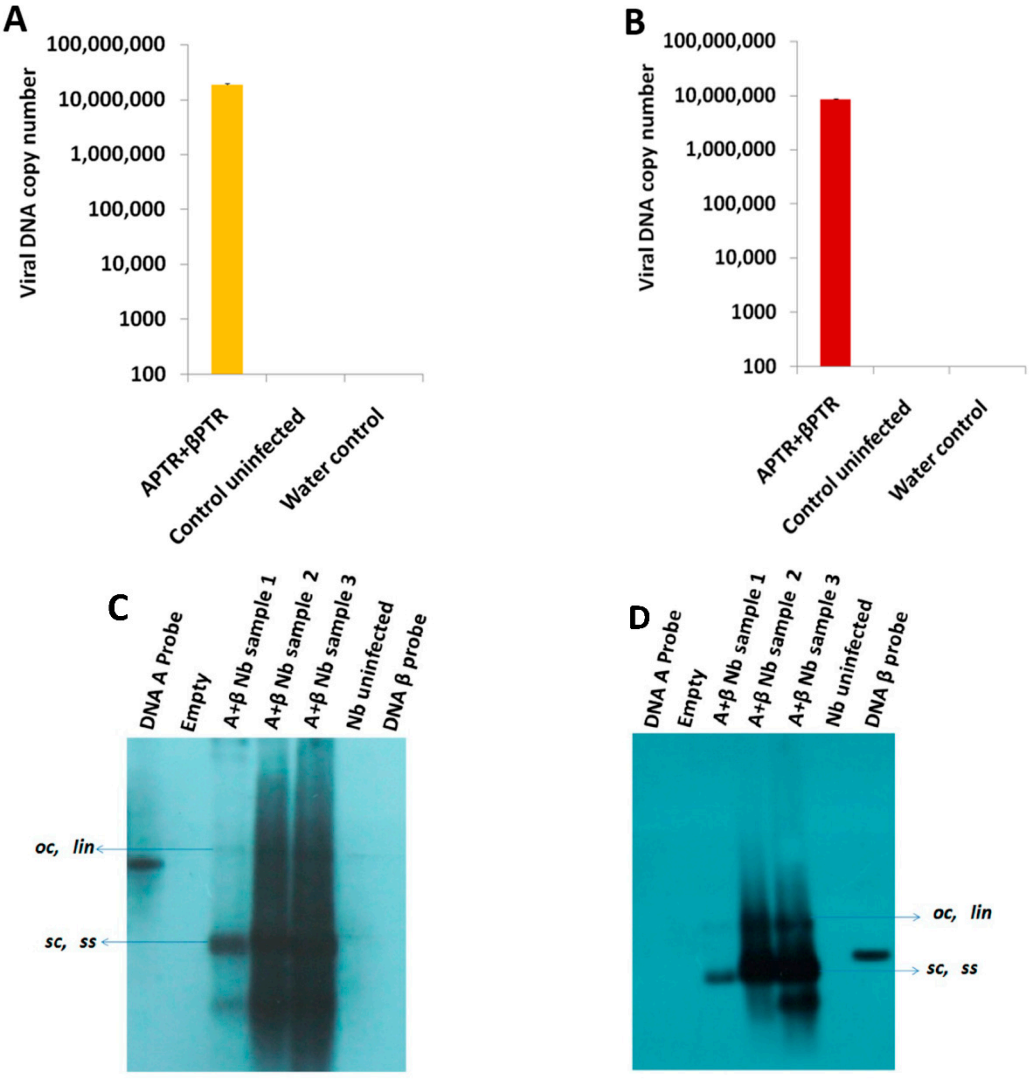

Figure 1. *Cont.*

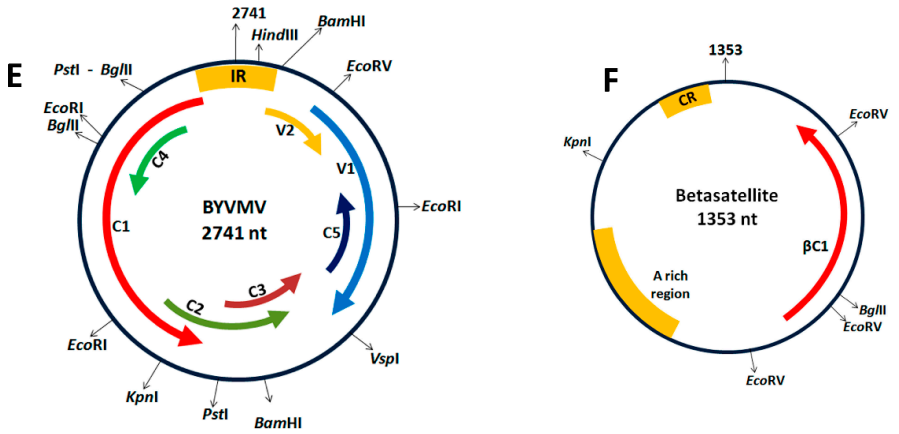

Figure 1. qPCR (quantitative PCR) to detect the copy number. Quantitative PCR was performed using 50 ng of viral DNA from APTR along with βPTR-infiltrated *N. benthamiana* plants using (**A**) BYVMV-specific primer (**B**) β satellite-specific primer. Southern confirmation of BYVMV accumulation with 5 µg of isolated viral DNA (**C**) using DNA A and (**D**) β satellite probe. Genome organization of *Bhendi Yellow Vein Mosaic Virus* (BYVMV) (GenBank: AF241479.1) (**E**) and associated β satellite (GenBank: AJ308425.1) (**F**). (oc—open circular, lin—linear, sc—super coiled, ss—single stranded, Nb—*N. benthamiana*, A+β—APTR + βPTR, IR—intergenic region, CR—conserved region, nt—nucleotides).

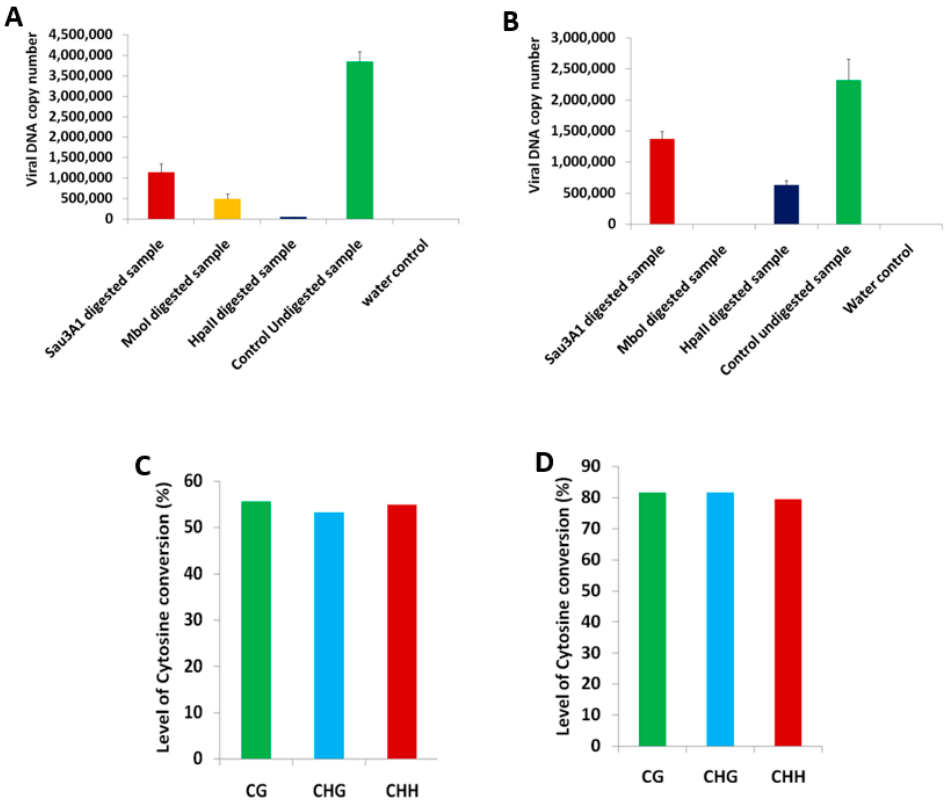

Figure 2. Quantitative PCR analysis of Methylation-sensitive enzyme-restricted products of BYVMV viral DNA from APTR along with βPTR-infiltrated *N. benthamiana*, with BYVMV specific primer (**A**) and β satellite specific primer (**B**). Level of cytosine conversion in Control DNA A sample (**C**) and Control DNA β sample (**D**), where different methylation bases are plotted against the level of cytosine conversion.

Table 1. List of primers used in the present study. The nucleotide substitutions are shown in bold face and underlined.

S. No	Primers	Sequences	Target DNA & Nucleotide Coordinate	Details of Experimental Use
1	BYVMV DNA A IR Forward	5′ GTTGACTATTTTTGAGACCCGATT 3′	BYVMV DNA (1–24)	Chop-PCR
2	BYVMV DNA A IR Reverse	5′ GGATCCCACATTTTTTGAATTG 3′	BYVMV DNA A (285–264)	Chop-PCR
3	*Bgl*II BYVMV AV2 Forward	5′ AGATCTATGTGGGATCCACTATTAAACG 3′	BYVMV DNA A (119–131)	Chop-PCR
4	*Hind*III BYVMV AV2 Reverse	5′ AAGCTTTCACATCCCCTTGGAACATCC 3′	BYVMV DNA A (485–465)	Chop-PCR
5	*Hind*III *BYVMV* C2 Forward	5′ AAGCTTATGCAGCATTCGTCTTTC 3′	BYVMV DNA A (1584–1601)	Chop-PCR
6	*Bgl*II *BYVMV* C2 Reverse	5′ AGATCTTTAGAGATATTTGAGGAC 3′	BYVMV DNA A (1170–1190)	Chop-PCR
7	*Bam*HI BYVMV AC4 Forward	5′ GGATCCTTATCTTTAAGAACTCTAAGAGC 3′	BYVMV DNA A (2130–2154)	Chop-PCR
8	*Hind*III BYVMV AC4 Reverse	5′ AGCTTATGAAAATGGGGAACCTCATCTTCACG 3′	BYVMV DNA A (2438–2412)	Chop-PCR
9	*Bgl*II BYVMV βC1 Forward	5′ AGATCTAATTATTATCTTATTATCAATAGTAC 3′	BYVMV DNA β (180–207)	Chop-PCR
10	*Hind*III BYVMV βC1 Reverse	5′ AAGCTTATGAAAATATCTATACATTTCATC 3′	BYVMV DNA β (602–578)	Chop-PCR
11	βC1 Promoter Forward	5′ ATAATGTGTGGATGAAATTTATAGA 3′	BYVMV DNA β 603–627	Chop-PCR
12	βC1 Promoter Reverse	5′ CTCATTTACCTATCGGTGTCTG 3′	BYVMV DNA β 1080–1059	Chop-PCR
13	BYVMV V2 RT Forward	5′ GCAACTTTTGTCGCAGGATT 3′	BYVMV DNA A (194–213)	Quantitative PCR
14	BYVMV V2 RT Reverse	5′ ATAGGCCTGTTTGTCCATGC 3′	BYVMV DNA A (406–425)	Quantitative PCR
15	BYVMV β RT Forward	5′ CGCGCGGTAAATGGTAAATA 3′	BYVMV DNA β (1017–1036)	Quantitative PCR
16	BYVMV β RT Reverse	5′ CTACGACGCGCGATATAACT 3′	BYVMV DNA β (1158–1177)	Quantitative PCR
17	C4 stop 1 Forward	5′ ATT TTCCTTCGAACTGGAT**T**AGCACGTGAAGATGAGGTT 3′	BYVMV DNA A (2386–2426)	Site-specific mutagenesis
18	C4 stop 1 Reverse	5′ AACCTCATCTTCACGTGCT**A**ATCCAGTTCGAAGGAAAAT 3′	BYVMV DNA A (2387–2426)	Site-specific mutagenesis
19	C2 stop 1 Forward	5′ CCGAGTACAACGGTTGGGT**T**AGAAAGACGAATGCTGCAT 3′	BYVMV DNA A 1563–1600	Site-specific mutagenesis
20	C2 stop 1 Reverse	5′ ATGCAGCATTCGTCTTTCT**A**ACCCAACCGTTGTACTCGG 3′	BYVMV DNA A 1600–1563	Site-specific mutagenesis
21	C2 stop 2 Forward	5′CGCTTCCTTGTGTTGAACTT**A**GATTGGTACCCGAGTACA 3′	BYVMV DNA A 1533–1571	Site-specific mutagenesis
22	C2 stop 2 Reverse	5′ TGTACTCGGGTACCAATC**T**AAGTTCAACACAAGGAAGCG 3′	BYVMV DNA A 1571–1533	Site-specific mutagenesis

High depth analysis on the control plasmid revealed a bisulfite conversion rate of 80–82% at 2 µg (Figure 2D) and of 53–55% at 4 µg of the template DNA (Figure 2C). The 53–82% bisulfite conversion may be due to different concentration and size of the plasmid which led us to keep 2 µg viral DNA as a constant for the bisulfite treatment, anticipating 99% conversion owing to less size of the BYVMV (2.7 kb) and β satellite (1.3 kb) than the control plasmids (pBlue DNA A 5.7 and pBlue β 4.3 kb). The viral DNA was isolated from the APTR- and βPTR-infiltrated *N. benthamiana* plant at 21 dpi. Two micrograms of viral DNA was subjected to bisulfite treatment and converted to concatemers by RCA (rolling circle amplification) for NGS. The NGS data was analysed with COV (Coverage distribution of methylation sites) and MET (Methylation profiling) modules of MethGo. The percentage of methylation sites covered in the target DNA sequence is a critical factor for evaluating the quality of the sequencing data. Methylation sites with high coverage should provide accurate methylation status. The COV module of Methgo extracts the coverage value for each cytosine from the post-alignment data and subsequently produces a reverse cumulative plot for methylation sites in CG, CHG and CHH context where H refers to A, C or T [28] (Figure 3A). The coverage map generated by the COV module had showed about 95% coverage of the cytosine methylation sites on the BYVMV viral genome with the 10× depth assuring the sequencing quality and data consistency (Figure 3A,B). Data analysis by Methgo tool revealed roughly 14–18% (Figure 3C) methylation of CG, CHH and CHG sites. This was considered as base level methylation when APTR along with βPTR were infiltrated.

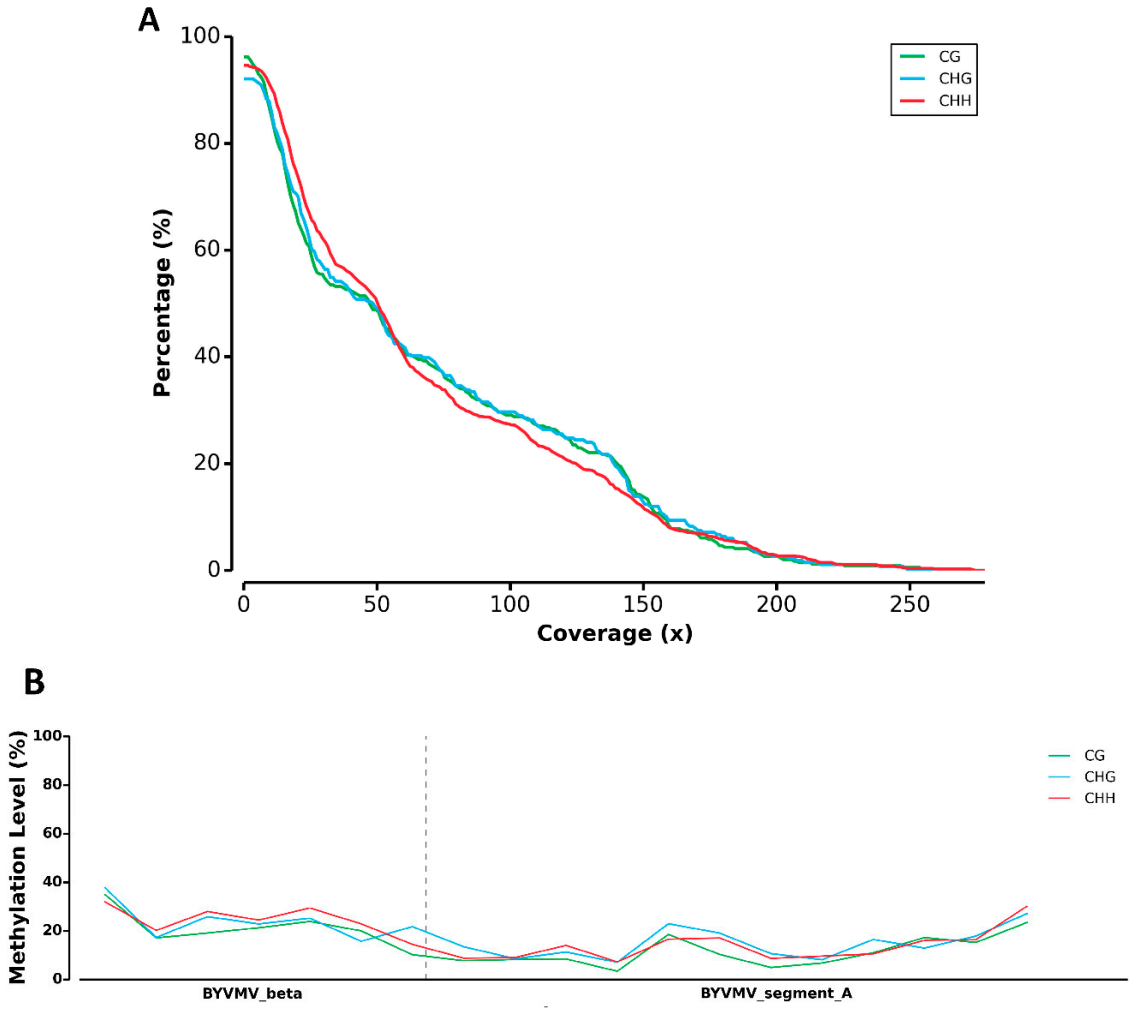

Figure 3. *Cont.*

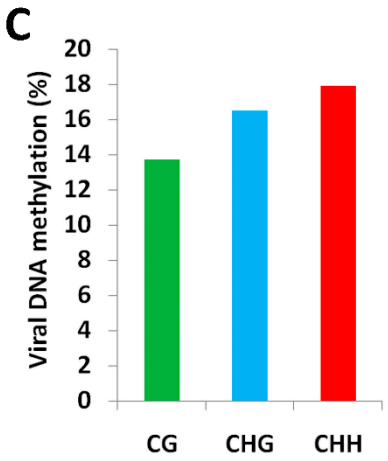

Figure 3. MethGo analysis of Bisulfite NGS Data for APTR and βPTR co-infiltrated plant samples: Coverage of methylation sites is a criterion for assessing the quality and reliability of methylation data. The COV module of MethGo software extracts the coverage for each cytosine from BS-Seeker alignment file and generates a reverse cumulative plot for methylation sites in CG, CHG and CHH context (where H refers to A, C or T). (**A**) Coverage map of 1 million Bisulfite NGS reads from APTR + βPTR co-infiltrated plant sample. *y*-axis represents the percentage of methylation sites covered in the BYVMV genome. *x*-axis represents the depth of coverage (*x*). (**B**) The genome-wide methylation map of BYVMV showing the level of methylation at different regions of BYVMV and β satellite. (**C**) Global methylation pattern of BYVMV genome derived from 1 million reads and represented by plotting different methylation bases against percentage methylation.

2.2. BYVMV Gene(s) Involved in Methylation Suppression

Based on the chop-PCR, qPCR and high depth analysis of bisulfite sequencing data, we assured that BYVMV genes or βC1 would have interfered with the DNA methylation. In order to identify whether BYVMV gene(s) were involved in TGS suppression, APTR alone infiltrated *N. benthamiana* plants were taken for further studies. The virus accumulation was confirmed by qPCR followed by Southern hybridization (Figure 4A,B). Chop-PCR was performed with various primers after digesting the viral DNA with MSREs and a significant reduction in amplification was found with at least one among the enzymes used when compared to the undigested one (Supplementary Figure S2). Chop-PCR analysis of 1.1 kb BYVMV genomic region which intervening between C4, V2 ORFs including IR, shows the complete absence of amplification in MSREs digested viral DNA samples. Interestingly, viral DNA copies determination by qPCR with MSREs digested viral DNA also demonstrates a more than 50% reduction in amplification, assuming that BYVMV genes should be involving in DNA methylation suppression (Figure 4C). In order to study the methylation pattern in an accurate manner, viral DNA isolated from APTR alone infiltrated *N. benthamiana* plants was subjected to bisulfite conversion and RCA. The concatamers were processed for Illumina sequencing as mentioned in the previous section.

The data that were analysed with one million reads by the MethGo software, which revealed approximately 4–5% methylation on a full-length BYVMV genome from the *N. benthamiana* plants, infiltrated with APTR alone (Figure 4D). Thus, we had confirmed the minimum level of DNA methylation in BYVMV. The coverage map generated by the COV module showed about 98% coverage of the cytosine methylation sites (Figure 5). Chop-PCR and high depth analysis of bisulfite reads inferred that BYVMV gene(s) were involved in the suppression of DNA methylation in βC1.

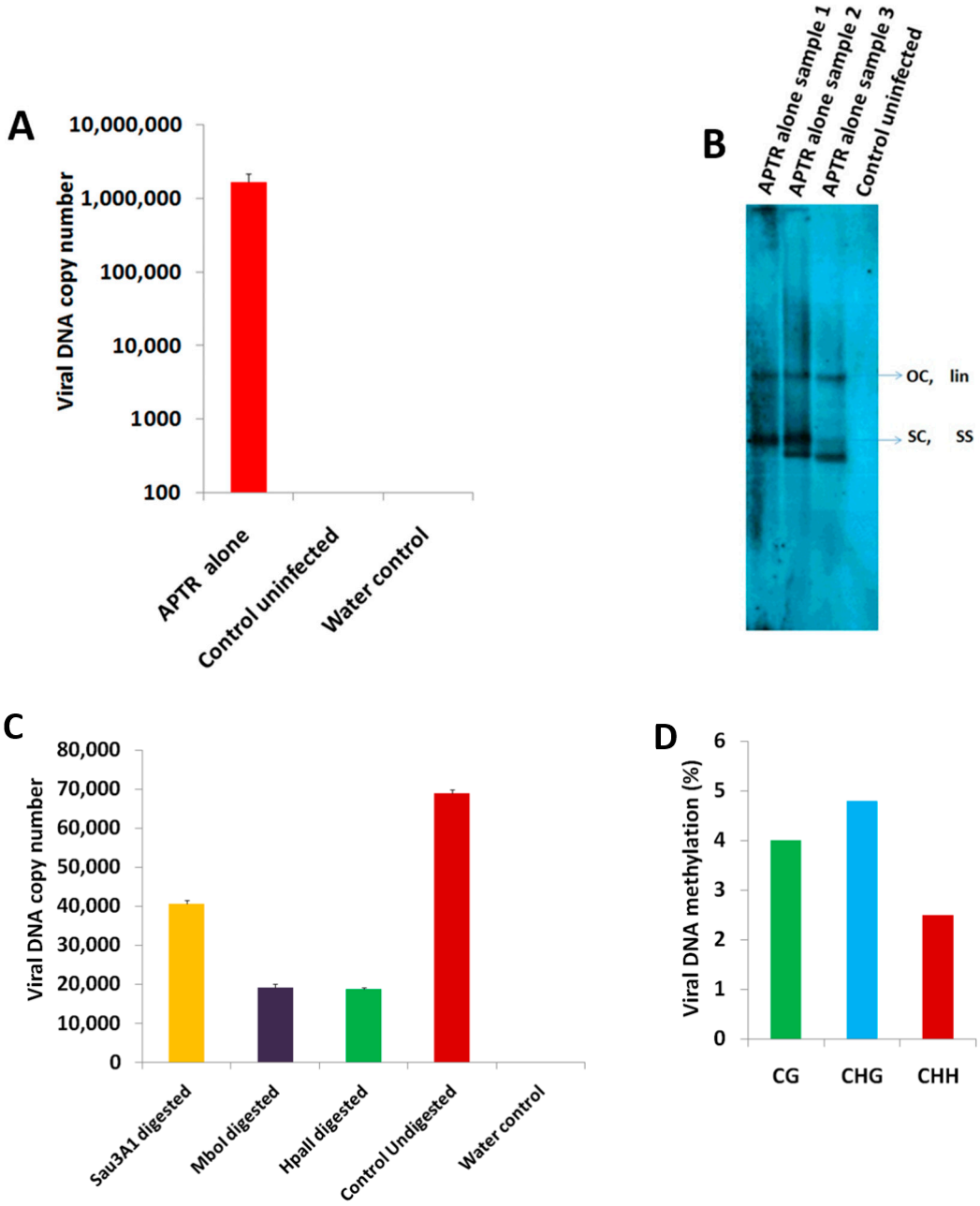

Figure 4. Confirmation of BYVMV DNA A accumulation in *N. benthamiana* plants. (**A**) qPCR of DNA derived from agroinfiltrated *N. benthamiana* with BYVMV-specific primers. (**B**) Southern confirmation of BYVMV in agroinfiltrated plants using DNA A probe. (**C**) Quantitative PCR of methylation-sensitive enzyme restricted products of viral DNA. (**D**) Global methylation pattern of BYVMV genome derived from 1 million reads and represented by plotting different methylation bases against percentage of methylation.

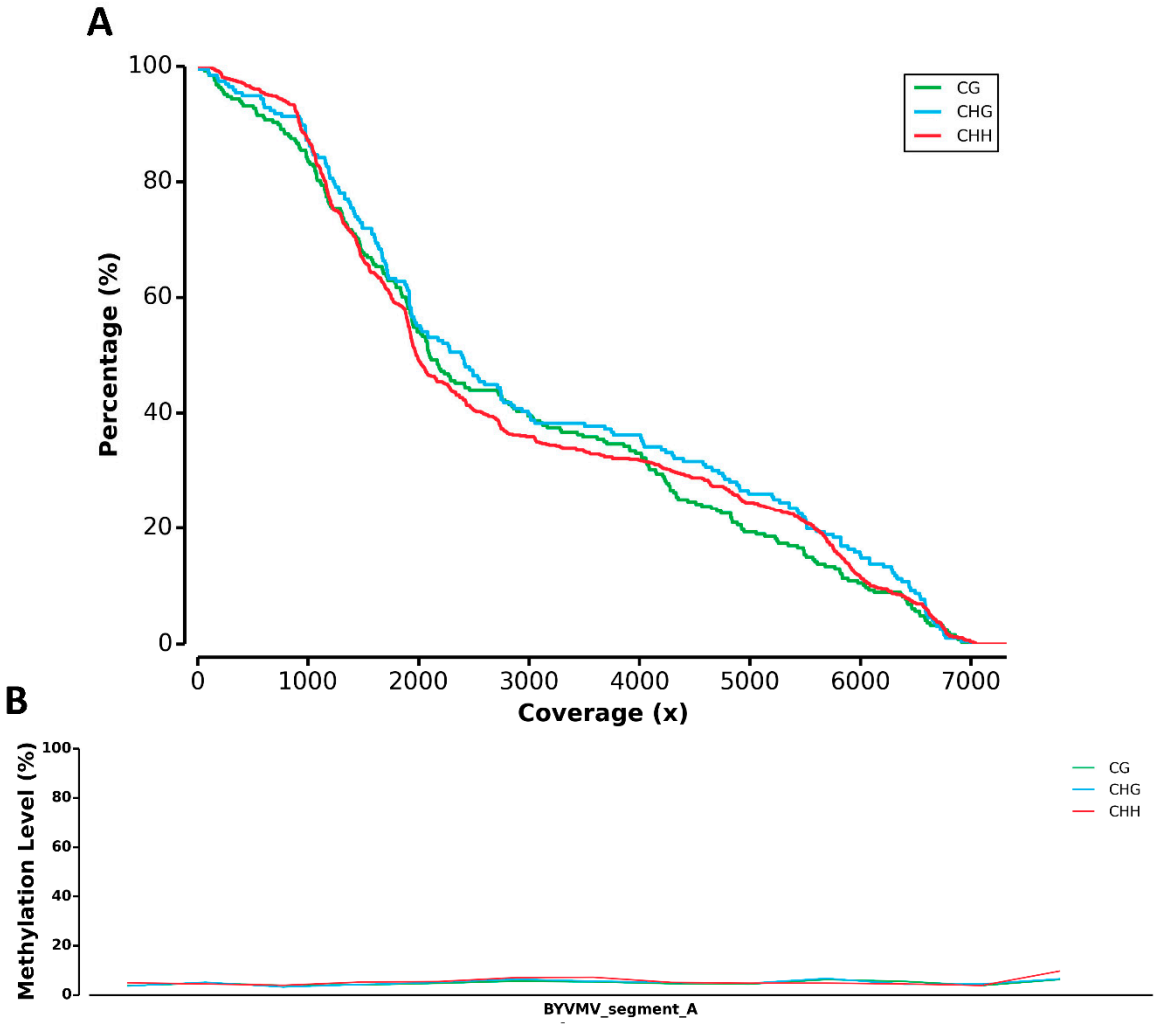

Figure 5. MethGo analysis of Bisulfite NGS Data for APTR alone infiltrated plant samples: (**A**) Coverage map of 1 million Bisulfite NGS reads. *y*-axis represents the percentage of methylation sites covered in the BYVMV. *x*-axis represents the depth of coverage (*x*) which indicates high quality and reliability of the outcome. (**B**) The genome-wide methylation map of BYVMV showing the level of methylation at different regions of BYVMV.

2.3. BYVMV C4 and C2 Hinders Transcriptional Gene Silencing

Analyses of the results of chop-PCR and bisulfite NGS showed that BYVMV genes act as suppressors of TGS. These genes are C2 and C4 of BYVMV, since they are known to exert various degree of PTGS interference activity. Therefore, in the present study, initially, C4was chosen for further exploration, since C4 is a proven suppressor of gene silencing (TGS and PTGS) and symptom determinant [22,29,30]. To analyse BYVMV C4's role in TGS suppression, a mutant APTR (C4MAPTR) was produced by introducing a stop codon at the N-terminal region of C4 ORF using mutagenic primers (Table 1, Primers 17 and 18) without disrupting the overlapping C1 ORF. This produces a premature truncated 10 amino acid sequence of C4. *N. benthamiana* plants, co-infiltrated with APTR and βPTR, showed leaf curling at 21 dpi while APTR alone infiltrated plants producing mild symptoms (Figure 6A and Table 2). As expected, C4MAPTR (PTR construct of C4 mutant 'A' DNA) alone inoculated *N. benthamiana* plants remained asymptomatic (Figure 6A and Table 2). It was surprising that all *N. benthamiana* plants infiltrated with C4MAPTR along with βPTR, were asymptomatic even at 40 dpi (Figure 6A).

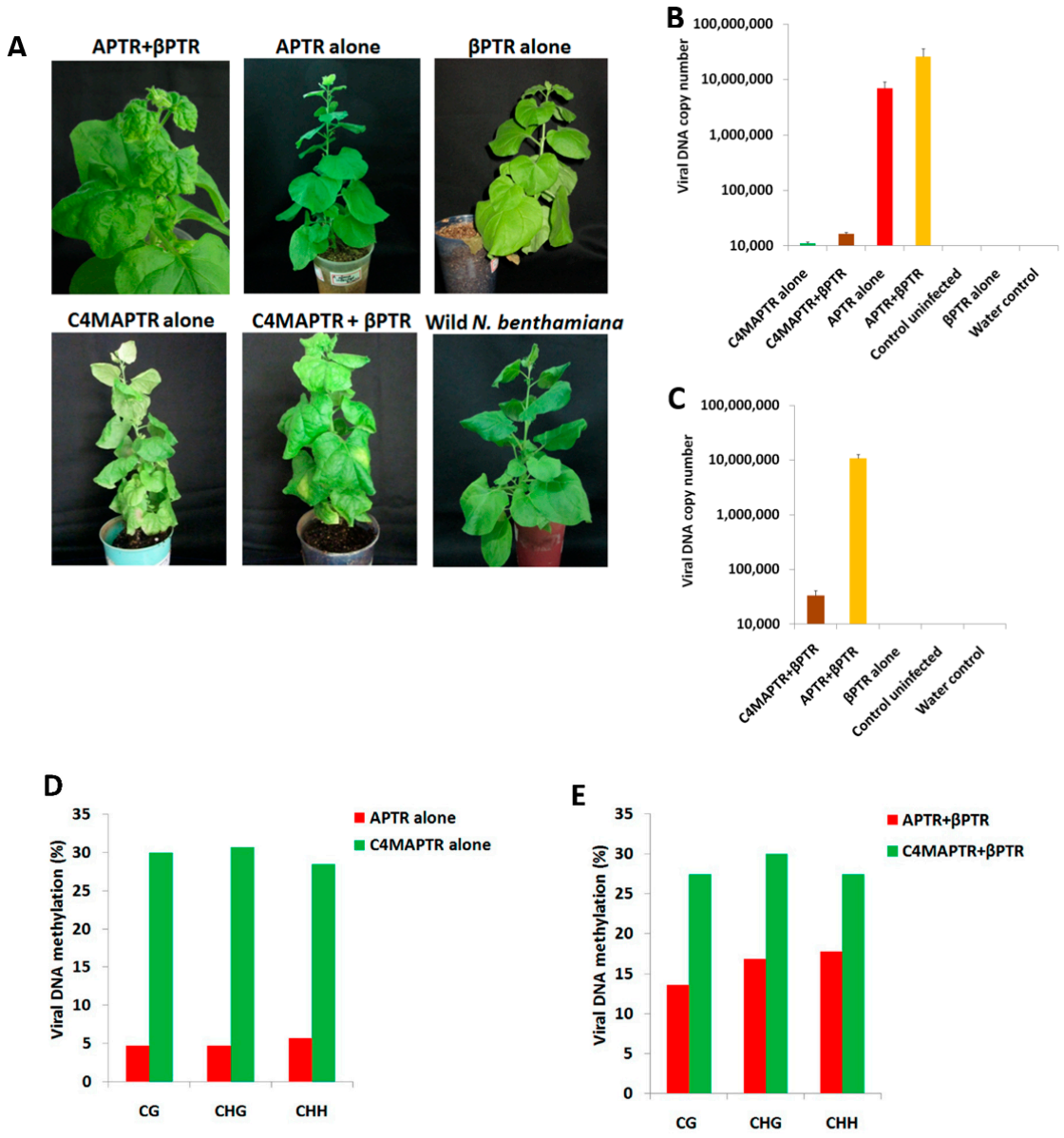

Figure 6. (**A**) Symptomatology of *N. benthamiana* plants infiltrated with various PTR constructs. Viral DNA isolated from plants of various PTR infiltrations, represented in Figure 6A, subjected to qPCR with BYVMV-specific primers (**B**) and β satellite-specific primers (**C**) showing viral DNA accumulation. Comparison of the global percentage of methylation among different methylation base contexts between viral DNA derived from APTR alone (**D**) infiltrated plants and C4MAPTR alone infiltrated plants, APTR + βPTR co-infiltrated plants and C4MAPTR + βPTR co-infiltrated plants (**E**).

Table 2. Agroinfiltration of *N.benthamiana* plants.

S.No	Type of Infiltration	Total No. of Plants Infiltrated	Severe Symptomatic Plants	Mild Symptomatic Plants	Asymptomatic
1	APTR alone	22	0	13	9
2	APTR + βPTR	27	13	4	10
3	C4MAPTR alone	10	0	0	10
4	C4MAPTR + βPTR	10	0	0	10
5	C2MAPTR alone	10	0	0	10
6	C2MAPTR + βPTR	10	0	0	10
7	βPTR alone	14	0	0	14

Viral DNA quantification by qPCR was done to explore the symptomatology of *N. benthamiana* plants infiltrated with C4MAPTR alone or C4MAPTR along with βPTR or βPTR alone. For all the infiltrated plants, DNA was extracted from all the leaves including the infiltrated leaves. As anticipated, APTR + βPTR inoculated plants showed higher viral DNA titre (2.5×10^7 copies) than APTR alone (6.9×10^6 copies) (Figure 6B,C). However, C4MAPTR alone (1.1×10^4 copies) or C4MAPTR along with βPTR-infiltrated plants (1.6×10^4 copies) showed fewer copies of viral DNA (Figure 6B,C). This suggests C4 is having additional function(s) for the virus survival by being involved in replication or cell to cell movement or TGS suppression. The viral DNA was extracted from C4MAPTR-infiltrated *N. benthamiana* plant leaves at 21 dpi. Bisulfite conversion and RCA were performed with this DNA. To know the methylation pattern, viral DNA from plant leaves infiltrated with APTR alone or APTR along with βPTR or C4MAPTR alone or C4MAPTR along with βPTR, were used for bisulfite NGS. Exploring the coverage map of APTR alone and APTR along with βPTR revealed 98% and 80% coverage of methylation sites with a depth of 100× and 10×, respectively. This was similar to C4MAPTR inoculated *N. benthamiana* samples except for coverage depth (Supplementary Figures S3 and S4). The bisulfite data analysis of the viral genome derived from *N. benthamiana* plants infiltrated with APTR alone (~0.6 million reads) or APTR along with βPTR (~0.7 million reads) showed consistent results that were observed in the previous data of wild type DNA infiltration (Figure 6D,E).

Intriguingly, the viral genome from plants infiltrated with C4MAPTR alone (~2.6 million reads) showed ~28–30% methylation compared to 4–5% methylation of the viral genome from plants infiltrated with APTR alone (Figure 6D). The viral genome from the *N. benthamiana* plants infiltrated with C4MAPTR along with βPTR (~2 million reads) revealed ~27–30% methylation compared to ~14–18% of APTR and βPTR together (Figure 6E). When C4MAPTR alone or C4MAPTR along with βPTR were infiltrated, the viral genome from the plants showed an altered level of methylation (~27–30%) compared to the infiltration of wild type constructs (~5–18%). These results imply that the genome of BYVMV becomes susceptible to methylation in the absence of C4, since C4 mutation renders inefficient suppression of DNA methylation (Figure 6D,E).

Previous reports confirmed BYVMV C2 as a strong transactivator and weak suppressor of PTGS [22]. It was also demonstrated that AC2/C2 effectively interfered with the DNA methylation by interacting with the methylation cycle proteins [15–18]. To evaluate the role of C2 on TGS impairment, the C2-deficient infectious construct (C2MAPTR) was infiltrated into *N. benthamiana* plants either as C2MAPTR alone or along with the β satellite (βPTR). All the C2 mutant construct- infiltrated plants were asymptomatic whereas the constructs of wild type BYVMV alone or BYVMV along with β satellite-infiltrated plants showed symptoms at 21 dpi [23] (Table 2). The qPCR analysis showed high accumulation of viral DNA in the plants infiltrated with APTR alone (7×10^6 copies) and APTR along with βPTR (1.3×10^7 copies) and less viral DNA accumulation in the plants infiltrated with C2MAPTR alone (5×10^3 copies) or C2MAPTR along with βPTR (9.1×10^5 copies) (Figure 7A,B).

In order to reveal the methylation profiles of the viral DNA from plants infiltrated with C2MAPTR alone or C2MAPTR along with βPTR, bisulfite NGS was performed. Coverage analysis of APTR alone or along with βPTR showed ~90% and 85% coverage of methylation sites with a depth of 200× and 10×, respectively. Similarly, we found 98% and 80% coverage of methylation sites for C2MAPTR alone or along with βPTR samples with a depth of 10× and 100×, respectively (Supplementary Figures S5 and S6). The analyses of the viral genome were done on ~0.6 million reads from plants infiltrated with APTR alone, ~0.7 million reads from plants infiltrated with APTR along with βPTR, ~2.8 million reads from plants infiltrated with C2MAPTR alone and ~3.2 million reads from plants infiltrated with C2MAPTR along with βPTR. The analyses showed 4–6% methylation of viral DNA in APTR alone infiltrated plants, 13–18% methylation of viral DNA in APTR along with βPTR infiltrated plants, 14–18% methylation of viral DNA in C2MAPTR alone infiltrated plants and 55–60% methylation of viral DNA in C2MAPTR along with βPTR infiltrated plants (Figure 7C,D). The MET module analyses of methylation pattern by MethGo showed an increased methylation of the viral genome when plants were infiltrated with C2MAPTR alone or C2MAPTR along with βPTR. This value is significant when

compared to the methylation values of the viral genome from plants infiltrated with APTR along with βPTR (Figure 7C,D). In conclusion, the viral genome methylation of plants infiltrated with C2MAPTR showed a higher value in the presence of β satellite, which signifies the higher level of C2 involvement in TGS suppression.

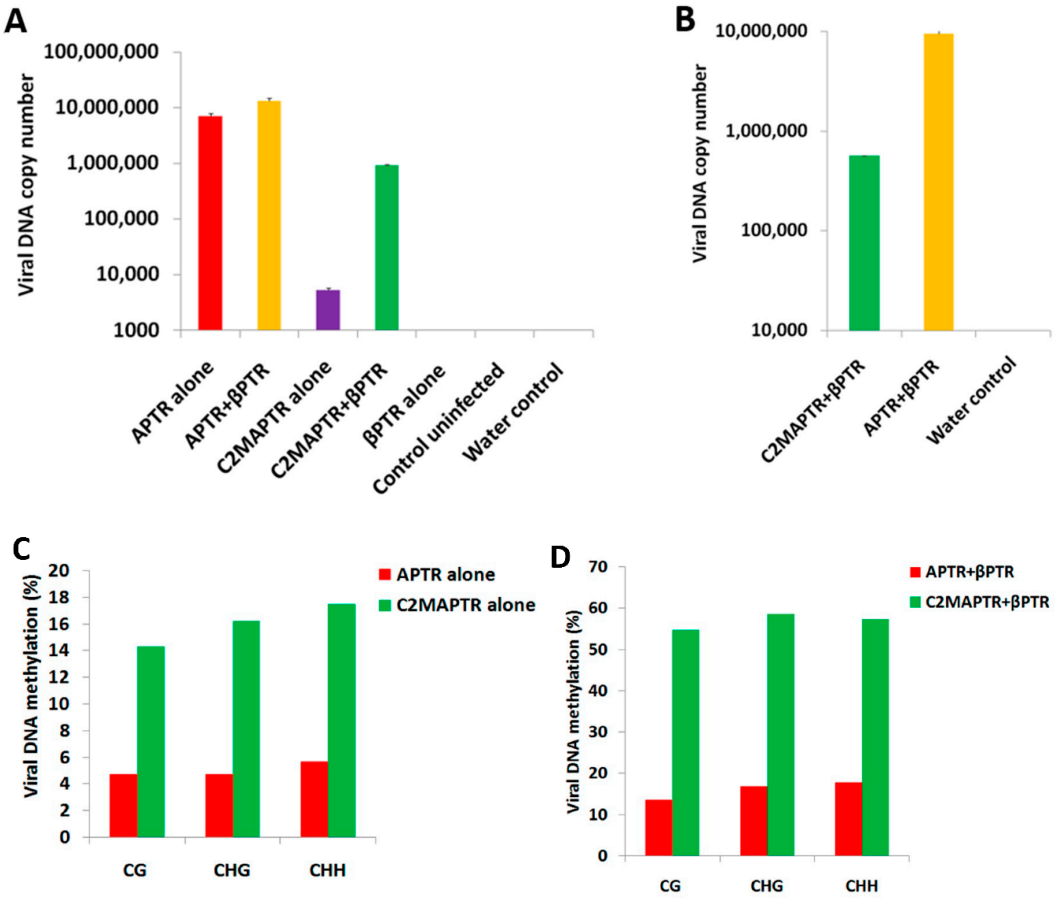

Figure 7. Copy number detection by qPCR. Viral DNA was isolated from the *N. benthamiana* plants infiltrated with various PTR constructs and copy number were determined using BYVMV-specific (**A**) and βsatelite-specific primers (**B**). Comparison of global percentage of methylation among different methylation base contexts between viral DNA derived from APTR alone infiltrated plants and C2MAPTR alone infiltrated plants (**C**), APTR + βPTR co-infiltrated plants and C2MAPTR + βPTR co-infiltrated plants (**D**).

2.4. C4 Mutation Impairs Viral Movement

Plants were infiltrated with APTR alone or APTR along with βPTR or C4MAPTR alone or C4MAPTR along with βPTR, to find out the influence of C4 on replication and movement. qPCR was performed on leaves harvested from the inoculated *N. benthamiana* and newly emerged leaves to determine the BYVMV viral DNA accumulation. In order to avoid the initial template of viral DNA raised from the agroiniltration, the enriched viral DNA was subjected to *Dpn*I digestion. Viral DNA quantification on inoculated leaves of *N. benthamiana* at 2 dpi showed prominent viral DNA accumulation in C4MAPTR-infiltrated leaves which was similar to APTR alone or along with βPTR (Figure 8A,C). On the other hand, qPCR results of the emerging leaves from the plants infiltrated either with C4MAPTR alone (32 copies) or C4MAPTR along with βPTR (54 copies) at 21 dpi showed less copies of viral DNA. (Figure 8B,D). These plants were asymptomatic too. However, when APTR alone or APTR along with βPTR was infiltrated into *N. benthamiana* plants, they showed a high level of viral accumulations in emerging leaves with mild or severe symptoms respectively at 21 dpi (Figure 8B,D).

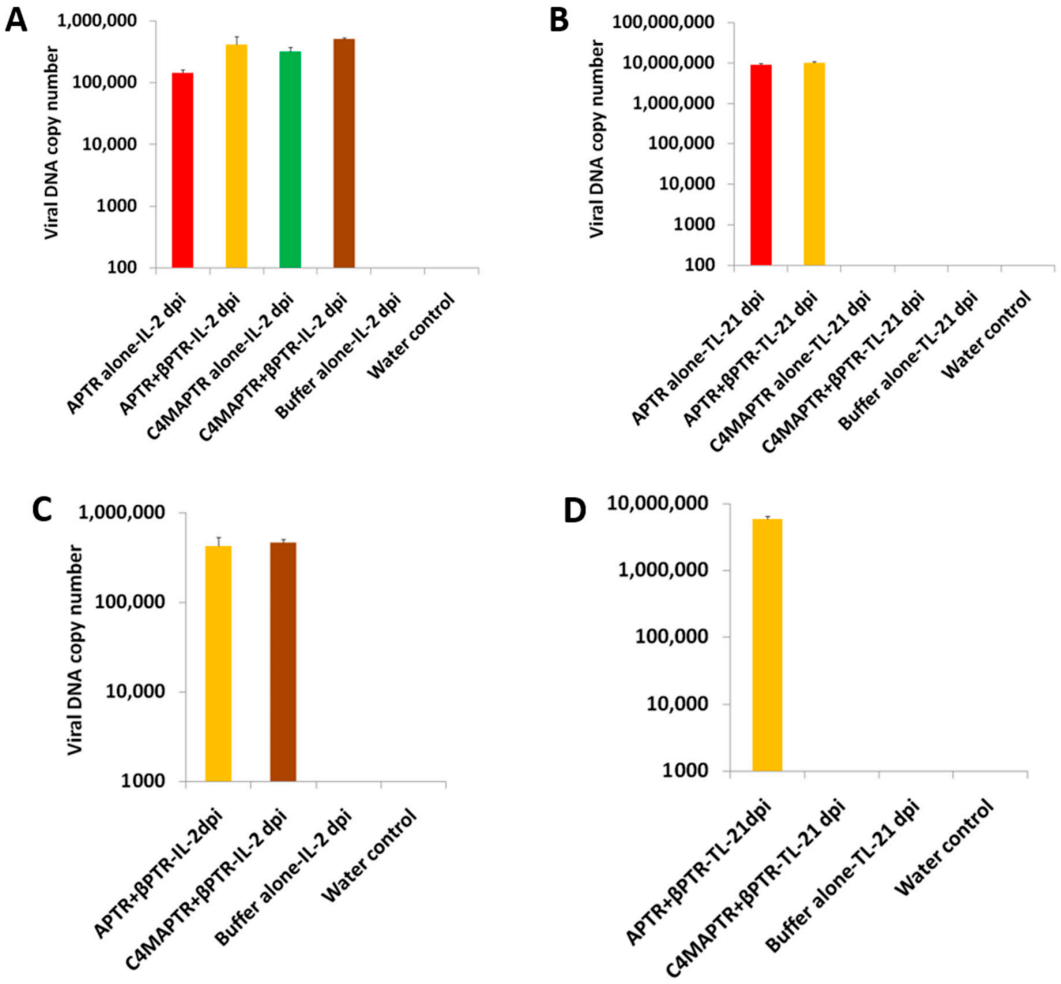

Figure 8. Copy number determination at different dpi. (**A**) BYVMV-specific primer mediated qPCR, showing the copy number of DNA A derived from *N. benthamiana* infiltrated with various PTR constructs of BYVMV at 2 dpi. (**B**) BYVMV-specific primer mediated qPCR, showing the copy number of viral DNA derived from *N. benthamiana* infiltrated with various PTR constructs of BYVMV at 21 dpi. (**C**) β satellite-specific primer mediated qPCR, showing the copy number of β satelite derived from *N. benthamiana* infiltrated with various PTR constructs of BYVMV at 2 dpi. (**D**) β satellite-specific primer mediated qPCR, showing the copy number of β satellite derived from *N. benthamiana* infiltrated with various PTR constructs of BYVMV at 21 dpi (IL—Infiltrated Leaf, TL—Top leaf, dpi—days of post infiltration).

The less viral DNA accumulation in emerging leaves of *N. benthamiana* must be due to the limited spread of virus movement. All these results confirmed the involvement of C4 in the movement of the virus in replication. Since it is established that C4 is involved in viral movement, its role in replication could be confirmed with a protoplast assay. Viral DNA accumulation in the protoplast was assessed with a standardised transfection protocol and viral DNA was extracted after 3 days of transfection followed by *Dpn*I digestion to remove the initial template caused by the transfection. The assessment of viral DNA quantity in protoplasts transfected with APTR alone or C4MAPTR alone or APTR/C4MAPTR along with βPTR, showed an increased value (Figure 9A,B). The increased quantity of viral DNA accumulation upon protoplast transfection with C4MAPTR alone or along with βPTR, suggests that C4 is not an impediment for viral replication. The assay with the emerging leaves and protoplasts confirms the involvement of C4 in viral DNA movement.

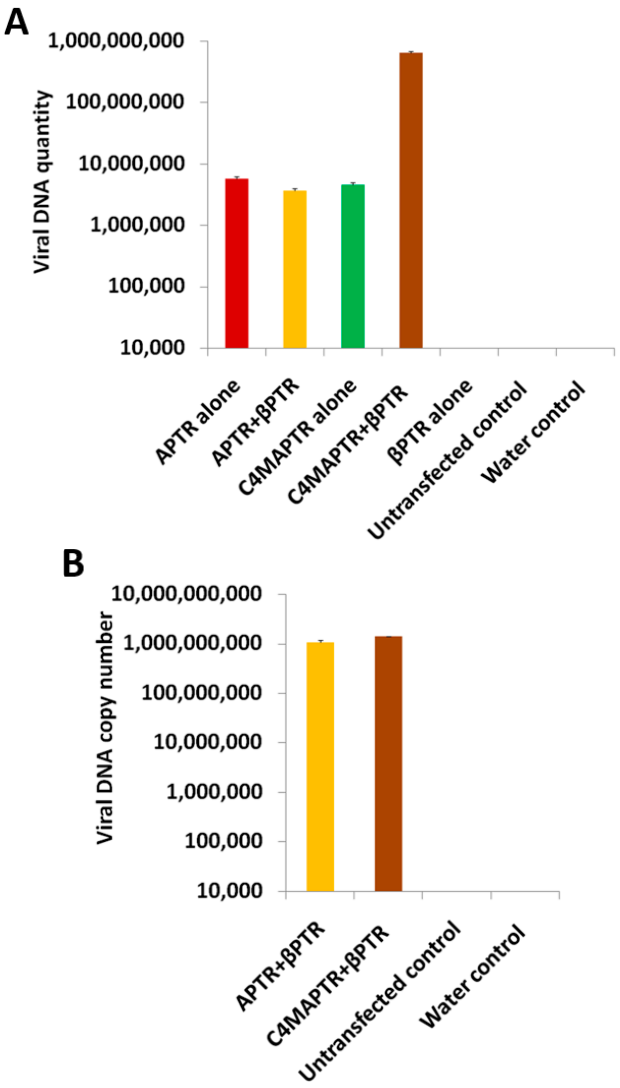

Figure 9. Evaluation of viral DNA accumulation in Protoplasts. Quantitative PCR using BYVMV-specific primer (**A**) and using β satelite-specific primer (**B**) showing the copy number of viral DNA from the mesophyll protoplasts of *N. benthamiana* when transfected with various PTR constructs of BYVMV.

3. Discussion

Small RNAs (sRNAs) produced by the plants are specific in targeting the RNA of the invading viruses as an endeavour of PTGS [31–33]. As a counter activity, geminiviruses encode an array of proteins (i.e., C2, C4, V2, C5 and βC1) which have the property to impair PTGS. It has been already established that BYVMV has three suppressors that are involved in PTGS hindrance. Further geminiviral double-stranded DNA intermediates are the potential target of RNA-mediated DNA methylation (RdDM) which is accomplished by short interfering RNAs (siRNAs). This in turn hinders geminiviral gene transcription and DNA replication at chromatin level. The notion that the repressive epigenetic mark of TGS established against geminiviral chromatin, comes from several lines of evidence which describe DNA methylation as an effective arm to hinder viral replication. However, the geminiviruses have a group of proteins—AC2/C2, V2, AC1 of begomoviruses and βC1 of β satellite [16,34–37] to counteract the TGS mechanism. Based on these observations, it was speculated that BYVMV, a monopartite geminivirus, should encode TGS suppressors. To evaluate BYVMV interference with the DNA methylation, the accumulation of BYVMV was assessed by qPCR

in the plants infiltrated with PTRs of BYVMV alone or along with β satellite and the C2 and C4 mutated genome. Chop-PCR analyses demonstrated that BYVMV gene(s) were involved in the prevention of methylation (Supplementary Figure S2). To substantiate the results of chop-PCR, high depth bisulfite sequencing was done. This confirmed that the viral genomes from plants, infiltrated with either BYVMV APTR alone or along with βPTR, were having less than 4–18% methylation. These data analyses clearly prove that BYVMV impaired the DNA methylation. Similar results were derived from *Tomato golden mosaic virus* (TGMV), *Beet curly top virus* (BCTV), *Tomato yellow leaf curl China virus* (TYLCCV) and *Tomato yellow leaf curl Sardinia virus* (TYLCSV) [16,17,34,35]. Almost in all cases, the conventional cloning method was used to predict the methylation level from 10–20 clones of viral DNA. In contrast, in the present study, we used NGS to generate a million reads to reveal the methylation status of the BYVMV genome, which providesa more consistent and accurate methylation level than traditional approaches.

The Previous studies with TYLCCV, *East African cassava mosaic Cameron virus* (EACMCV) and *African cassava mosaic virus-Cameron* (ACMV-CM) confirmed the role of C4 in symptom production and suppression of PTGS [27–29]. Hence, the C4 mutant BYVMV (C4MAPTR) was taken for initial studies. However, the C4MAPTR-infiltrated *N. benthamiana* plants remained asymptomatic even when it was infiltrated along with cognate β satellite (βPTR), which is known for its symptom severity [19,22]. The qPCR of the viral genome derived from plants infiltrated with C4MAPTR alone (1.1×10^4 copies) or C4MAPTR along with βPTR (1.6×10^4 copies), showed lower viral DNA accumulation than wild type PTR constructs (Figure 6B,C). The analysis of methylation profiles using MethGo showed ~28–30% methylation of the viral genome from plants infiltrated with C4MAPTR alone or C4MAPTR along with βPTR (Figure 6D,E). This suggests that C4 is involved in the suppression of TGS. Earlier, it had been shown that the C4-deficient TYLCV-Sardinia and *Tomato leaf curl virus* (ToLCV-Australia) remained infectious with a significant difference in symptoms compared to the wild type virus [38]. Consequently, it has been shown that BCTV or ToLCV-Australia C4 produced virus-like symptoms when expressed in transgenic tobacco or tomato [39,40], representing C4 participation in symptom development. In the present work, BYVMV C4 was studied and demonstrated for its role in symptom determination, as observed in earlier studies. Further, its role in TGS suppression was also studied since the suppression of DNA methylation and the reversal of TGS by C4 was reported only with a natural recombinant begomovirus (Y194) infecting *Malvastrum coromandelianum*. The Y194 C4 is almost identical (84 out of 85 amino acids) to that of *Pepper leaf curl china virus* (PepYLCCNV) and the nucleotide sequence except the C4 gene has ~97% identity with TYLCCNV [29]. The DNA methylation suppressor activity of C4 from Y194 virus has been elucidated by analysing the 25 bisulfite clones which represent the methylation status in the particular 366 nt long viral DNA fragment. Whereas in the present study, the DNA methylation suppressor activity of BYVMV C4 has been proved by analysing ~2.6 million bisulfite reads from C4MAPTR alone and ~2 million reads from C4MAPTR along with βPTR infiltrated samples. It is interesting to note that millions of BYVMV reads were mapped with all over its genome which in turn gave a highly accurate methylation status. When compared to ~4–18% viral DNA methylation level of either APTR alone or APTR along with βPTR samples, ~28–30% of viral DNA methylation with either C4MAPTR alone or along with βPTR confirms the role of BYVMV C4 in viral DNA methylation suppression. When the C4 mutant constructs infiltrated in *N. benthamiana* plants either alone or along with β satellite, the emerging leaves were totally devoid of BYVMV accumulation. In addition, the protoplast assay with C4MAPTR showed the retention of replication potential like APTR. This confirmed that C4 was not an impediment for viral DNA replication but was involved in the viral movement. In monopartite begomoviruses, the V1 might have NSP activity as had been reported *in Tomato leaf curl virus*, Israel (TYLCV-Is). In TYLCV-Is the CP was localized in the nucleus which retained the import and export processes [41–43]. The CP of TYLCV-Is also displayed a high affinity toward ssDNA molecules with slight binding property with double-stranded DNA (dsDNA) [43]. It has both nuclear localization signal (NLS) and nuclear exporting (NES) signal which enable the nucleo-cytoplasmic transport of TYLCV DNA [41,43]. Similarly, the CP of BYVMV was also

found to be localized in the nucleus since it has NLS and NES [44]. However, there is an ambiguity regarding the proteins involved in movement. The earlier reports had proposed that V2 or C4 might act as movement protein (MP) without concrete evidence [38,41,45,46]. Based on these results, we are proposing that BYVMV C4 should act as an MP. This has to be confirmed by performing DNA binding, cellular localization and protein-protein interaction studies with the C4 and CP.

Previously, it had been shown that AC2/C2 of TGMV/BCTV could perturb TGS and drastically reduce the plant DNA methylation by inactivating Adenosine kinase (ADK) of the methyl cycle [34,35,47]. In yet another mechanism, it had been confirmed that C2 functioned as an impediment for the proteasome-mediated degradation of *S*-adenosyl-methionine decarboxylase 1 (SAMDC1) [35]. This led to acute disturbance in the balance between S-adenosine methionine (SAM) and decarboxylated S-adenosine methionine (dcSAM). Based on these observations of AC2/C2 role in TGS interference, BYVMV C2 was selected for further exploration, since it had already demonstrated to be a strong transactivator and a week suppressor of PTGS [22]. Indeed, the C2 mutation led to a drastic reduction in the viral DNA accumulation (Figure 7A). High depth bisulfite sequencing analysis demonstrated that C2 was a suppressor of TGS like the AC2/C2 of TGMV, BCTV and BSCTV [35,48]. However, C2MAPTR along with βPTR-infiltrated *N.benthamiana* plant showed 55–60% methylation, which is higher than C4MAPTR alone or along with βPTR (28–30%). The exact reason remains to be deciphered for the presence of hypermethylation on viral DNA upon C2MAPTR along with βPTR infection. Probably itmay be due to viral DNA accumulation or other reasons. The BYVMV C2 mutation had reduced the viral DNA accumulation by producing hypermethylation on the BYVMV genome in CG, CHG and CHH context (Figure 7C,D). This suggested that C2 had influenced the common methylation cycle than a particular methyltransferase activity. It is interesting to note that βC1 had been shown to impair the TGS by inhibiting the activity of S-adenosyl homocysteine hydrolase (SAHH) [18]. However, BYVMV βC1 did not have any role on the TGS interference, since C4MAPTR or C2MAPTR inoculated along with βPTR revealed hypermethylation. Though TGS suppressor activity was exhibited by C2 and C4, the symptom production and viral DNA accumulation was lesser when *N. benthamiana* plants were infiltrated with APTR alone than APTR along with βPTR. This is because βC1 is a multifunctional protein, known to play a stronger role in PTGS suppression and symptom determination than C2 and C4 [22]. Further it also interacts with many host proteins and enhances viral DNA accumulation and symptom production [25,49]. Hence, it is concluded that the effective infection in host plants is governed by a cumulative activity of C2, C4 and βC1.

4. Materials and Methods

4.1. Cloning

pAPTR4 plasmid containing full-length DNA-A of BYVMV (2741 nt) (GenBank Accession No: AF241479.1) [19] was used for making a mutation in the *N*-terminal of C4 ORF. The entire C4 ORF lies within the C1 ORF under the complementary reading frame (Figure 1E). A stop codon was introduced in the N-terminal of C4 ORF at the 11th amino acid (UCA to UAA) by a single nucleotide change by using mutagenic primers (Table 1, Primers 17 and 18) without affecting the C1 coding sequence. The PCR conditions and *Dpn*I digestion were performed as per the manufacturer's instructions (Thermo Scientific, Waltham, MA, USA). The plasmid containing the specific mutation in the N-terminal of C4 ORF was selected and named as pKK1.The full-length BYVMV containing the mutated C4 sequence was released from pKK1 by *Eco*RV and *Sac*I digestion and the resulting 2.7 kb BYVMV fragment was cloned in the same restriction sites of pAPTR5. Thus, 1.9 mer APTR plasmid was created and the plasmid was renamed as pKK2. A 600 bp fragment containing the intergenic region (IR) and a part of C1 and V2 ORF was released from pOK12 [50] 0.2 mer A DNA plasmid [23] by *Sac*I and *Eco*RV digestion. This 600 bp fragment was cloned in pKK2 on the same restriction sites and the resulting clone was named as pKK3 1.2 mer. This pKK3 clone contains PTR on both sides of the BYVMV. The entire 1.2 mer APTR was released from pKK3 by *Sal*I and *Sac*I digestion and the

released fragment was cloned into pBIN PLUS vector at the corresponding sites. The resulting plasmid was renamed as pBIN-C4MAPTR, mobilized to *Agrobacterium* strain EHA 105 by triparental mating and then used for agroinfiltration experiments [51].

pCAMBIA C2MAPTR construct was created by Sam Aldrin [23]. Briefly, two stop codons were introduced in the N-terminal region of C2 by using mutagenic primers (Table 1, Primers 19–22). C2 mutations were introduced in the pAPTR4 plasmid which contained full length A DNA. In C2 ORF, the seventh serine residue and tenth lysine residue was converted into stop codons. pAPTR4 containing two C2 mutations was digested with *Eco*RV and *Sac*I and cloned in pAPTR5 to produce pC2mut-APTR6, which contains a wild type copy of C2 ORF. In order to remove the wild type C2, a 600 bp BYVMV fragment was released from pOK 0.2 mer by digestion with *Eco*RV and *Xho*I and cloned into pC2MAPTR6 at the site of *Eco*RV and *Sal*I. This created pBKS 1.2 mer C2MAPTR. The pBKS 1.2 mer C2MAPTR was digested with *Sac*I and *Xho*I and cloned into pCAMBIA 2301 at the site of *Sac*I and *Sal*I to produce pCAMBIA-C2MAPTR (C2MAPTR). All the clones were confirmed by restriction digestion.

4.2. Agroinfiltration

The PTR constructs of BYVMV was mobilized into *Agrobacterium tumefaciens* strain LBA 4404 or EHA 105 by triparental mating. Agroinfiltration was performed as reported previously [22,31]. Briefly, the transconjugants were grown in 50 mL of AB broth (AB media salts + AB media Buffer + Glucose (0.5 g/100 mL)) with the respective antibiotics (Rifampicin—10 µg/mL, Kanamycin—50 µg/mL) and 100µM Acetosyringone. The cells were pelleted by centrifugation at 6000 rpm for 5 min at 0.5 OD_{600}. The pelletted culture was then resuspended in an infiltration medium [10 mM $MgCl_2$, 10 mM MES pH 5.5, Acetosyringone (100 µM)]. The wild type *N. benthamiana* plants were used for the infiltration studies. For co-infiltration, each *Agrobacterium tumefaciens* culture was grown up to OD_{600} 0.5 and equal volume was mixed prior to infiltration.

4.3. Viral DNA Isolation

Viral DNA was extracted from the total leaves (both the infiltrated and non-filtrated leaves) or specifically infiltrated leaves of *N. benthamiana* by CTAB-alkaline lysis method [52]. 1 g of *N. benthamiana* leaf sample was ground with liquid N2 and thoroughly mixed with 10 mL of 2× CTAB. The ground homogenous mixer was transferred to 2 mL tubes and kept at 60 °C for 5–10 min to neutralize the degrading enzymes. The samples were brought to room temperature and the total DNA was isolated via conventional Chloroform: Isoamyl alcohol (24:1) wash and absolute alcohol precipitation method. The final aliquot was resuspended in 200 µL of 0.1×Tris-EDTA (TE) buffer pH 8. In the case of viral DNA isolated from infiltrated leaf, the samples were treated with a *Dpn*I enzyme to remove the initial template coming from the bacteria. With this aliquot 400 µL of freshly prepared 1% SDS and 0.2 M NaOH solution was added. The contents were mixed thoroughly and kept on ice for 15 min. With these contents 300 µL of 3 M sodium acetate (pH 5.2) was added. The contents were mixed gently and kept on ice for 30 min. The tubes were centrifuged at 10,000 rpm for 10 min at 4 °C and the top supernatant was transferred to a new tube. Along with this content, an equal volume of absolute alcohol was added and mixed well. The solution was kept for precipitation at −20 °C for 2 h. The tubes were centrifuged at 12,000 rpm for 10 min at 4 °C. The top supernatant was removed and the pellet was washed with 70% alcohol and vacuum dried. The pellet was resuspended with sterile double distilled water. With this aliquot one half volume of 7.5 M Ammonium acetate and 2.5 volume of absolute alcohol was added. The contents were mixed gently and kept for overnight precipitation at −70 °C. The tubes were centrifuged at 12,000 rpm for 10 min and the supernatant was removed. The pellet was washed with 70% alcohol and dried under a vacuum. Finally, the pellet was thoroughly resuspended with 20 µL of sterile double-distilled water and 2 µL of the sample was used for PCR analysis.

4.4. Chop-PCR

Three Methylation-Sensitive Restriction Enzymes (MSREs) such as *Sau3AI*, *MboI*, and *HpaII* were selected for chop-PCR. The BYVMV viral DNA isolated from the infiltrated plants was quantified by fluorimetry using Hoechst 33258 dye and an equal quantity of viral DNA was digested with MSREs. 300 ng of isolated viral DNA was digested with 10 units of each MSRE with a total volume of 20 µL per reaction. For each reaction mixture, buffers specific to the enzyme were used at 1× final concentration and incubated at 37 °C for 3 h. For control, the same quantity of DNA was taken without the enzyme. PCR was performed by taking an equal quantity of digested and undigested viral DNA samples as templates with various primers (Table 1) and proper controls.

4.5. Southern Hybridization

Isolated viral DNA was quantified using a fluorescent Hoechst 33258 dye. 5 µg of isolated viral DNA from each plant sample was loaded on 0.8% agarose gel and electrophoresed at 100 V in 1× TNE buffer (40 mM Tris-acetate, pH 7.5, 20 mM sodium acetate and 2 mM EDTA) [53,54]. After electrophoresis the gel was treated with 250 mL of denaturation solution for 30 min under constant shaking. The gel was washed with sterile water and treated with 250 mL of neutralization solution by keeping it under constant shaking for 30 min; DNA was further transferred on to the Biobond^{TM} nylon transfer membrane (Sigma-Aldrich, St. Louis, MO, USA) (using 20× SSC (Saline Sodium Citrate buffer—0.3 M $Na_3C_6H_5O_7$, 3 M NaCl pH 7.0). The hybridization, labeling and detection of nucleic acid was carried out by following the instructions from Alkphos' direct labelling and detection system (GE Healthcare, Buckinghamshire, UK).

4.6. Quantitative PCR (qPCR)

Absolute quantification of the viral DNA was done by standard curve method using ABI 7000 sequence detection systems from Applied Biosystems, Foster city, CA, USA. Standards were prepared by using plasmids having a single copy of the viral DNA genome which was used for making serial dilutions from 10^6 to 10^9. The real-time PCR master mix contains 1× SYBR green mix, target sequence-specific forward and reverse primers at 10 pM concentration, Template DNA (50 ng) and sterile double–distilled(dd) water to make the total volume 20 µL. PCR cycling parameters include 1 cycle of 50 °C for 2 min, 1 cycle of 95 °C for 3 min, 40 cycles each of 95 °C for 15 s followed by 60 °C for 1 min. The viral copy number was determined on the basis of threshold *C*t values. A dissociation curve was chosen for the reaction specificity assessment using target DNA-specific peaks. Three biological samples were taken in triplicates to get consistent values and data were analysed using ABI PRISM 7000 system SDS software (Thermo Scientific, Waltham, MA, USA).

4.7. Protoplast Isolation and Transfection

Protoplast isolation and transfection were done by following the Sheen lab protocol [55]. Leaf mesophyll protoplast was isolated from 4–6 weeks old *N. benthamiana* plant leaves by using cellulase onozuka R-10 and Macerozyme R-10. The enzyme solution was prepared by dissolving 1.5% cellulose R10 (*w*/*v*), 0.4% Macerozyme R10 (*w*/*v*) and 20 mM KCl in 20 mM MES pH 5.7. The solution was incubated at 55 °C for 10 min to inactivate the DNase, protease and increase the enzyme solubility. The mixture was cooled to 25 °C and 10 mM $CaCl_2$ and 0.1% BSA was added and dissolved completely. The final clear and light brown colour enzyme solution was filtered into a clean petridish using a 0.45 µm syringe filter. The leaf blade was finely cut into small strips using a sharp blade and the leaf strips were immediately immersed in the enzyme mixture without delay. This setup was kept undisturbed under a vacuum and dark conditions for 3 h. After incubation, the enzyme solution containing the protoplasts was gently swirled and filtered using a fiber mesh. The isolated protoplasts were washed with W5 solution (154 mM NaCl, 125 mM $CaCl_2$ and 5 mM KCl dissolved in 2 mM MES pH 5.7) and counted using Haemocytometer. The protoplasts were diluted to the desired

concentration using MMG (0.4M Mannitol, and 15 mM $MgCl_2$ dissolved in 4 mM MES pH 5.7) solution and 2 $\times$ 10^5 cells were taken for transfection of each plasmid construct.

The PEG-$CaCl_2$ (0.2 M mannitol, 100 mM $CaCl_2$ dissolved in 40% PEG 4000 (w/v)) solution was used for protoplast transfection. The transfection mixture was prepared by adding 7 µg of plasmid DNA (various PTR constructs of BYVMV), 2 $\times$ 10^5 protoplasts with a total volume of 100 µL, 50 µg of calf thymus DNA (Carrier DNA) and 110 µL of PEG-$CaCl_2$ solution in a clean 1.5 mL tube. The transfection mixture was mixed completely by tapping gently and kept undisturbed at 25 °C for 20 min.After incubation, the mixture was washed with W5 solution and the cells were recovered by centrifugation at 100$\times$ *g* for 2 min. The pellet containing transfected protoplasts was resuspended in WI solution and incubated for 3 days.After the incubation period, the protoplasts were lysed and total DNA was isolated by 2$\times$ CTAB method. The isolated DNA was treated with *Dpn*I to degrade the initial template arising from the transfection. Further DNA was subjected to chloroform: Isoamyl alcohol wash twice and precipitated with absolute alcohol. The final aliquot was resuspended in 0.1$\times$ TE buffer pH 8. Absolute quantification of viral DNA was done by standard curve method by taking 50 ng of total DNA from each sample.

4.8. Bisulfite Conversion

Bisulfite conversion of viral DNA was performed using an Epitect bisulfite conversion and cleanup kit (Cat. No: 59104, Qiagen, Hilden, Germany). Specific kit buffers were diluted with ethanol as per the manufacturer's recommendations. Since the bisulfite method solely depends on the complete conversion of cytosine and the complete non-conversion of 5-mC, initially, we decided to compare the sensitivity of the method by utilizing different sizes of DNA plasmid and concentration by keeping the kit manufacturer's recommended temperature (60 °C) as constant. Towards achieving an effective conversion rate, we transformed pBlue Script II plasmid containing full-length BYVMV (pBlue DNA A, 5.7 kb) or β satellite (pBlue β, 4.3 kb) into a methylation-deficient *E. coli* strain ET12567 (*dcm*$^-$*dam*$^-$*hsdM*$^-$). Various concentrations of plasmids (0.5, 1, 2 and 4 µg) isolated from ET12567 were subjected to bisulfite conversion without shearing the DNA. The DNA thus converted was subjected to rolling circle amplification (RCA) with the random primers as described earlier [56]. A prominent amplification was found only with 2 or 4 µg concentration and the concatemers were submitted for NGS (refer Sections 4.10 and 4.11). The output data was analysed with MethGo software (refer Section 4.11) for graphical representation of the methylation level of different genomic regions of BYVMV; it was concluded that 2 µg DNA was optimal for the bisulfite conversion.

The bisulfite reaction components consist of 2 µg of the viral DNA sample (with total volume of 20 µL), 85 µL of bisulfite mix, 35 µL of DNA protect buffer and RNase free water to make the final volume of 140 µL. The DNA protect buffer was turned from green to blue upon resuspending the DNA-bisulfite mix, which indicated sufficient mixing and the correct pH. For bisulfite conversion, a separate PCR protocol was followed as per the kit manual. The PCR cycle has an alternate cycle of denaturation and incubation which includes 5 min at 95 °C, 25 min at 60 °C, 5 min at 95 °C, 85 min at 60 °C, 5 min at 95 °C, 175 min at 60 °C and an indefinite hold at 20 °C. The DNA clean-up steps were performed by following the protocol from the kit manual using DNA extraction columns and buffers given with the kit. Following conversion, desulphonation and washing steps, the final aliquot of DNA was eluted using an elution buffer with a total volume of 20 µL and then immediately used for RCA [56].

The methylation-deficient *E. coli* strain ET12567 (*dam*$^-$*dcm*$^-$*hsdM*$^-$) was used to get the unmethylated control DNA for the bisulfite experiment. Further, a plasmid containing the full length genome of β satellite was transformed to ET12567 and the transformant colonies were selected on suitable antibiotic agar media. The β satellite plasmid isolated from the ET12567 was confirmed by restriction digestion and used as unmethylated DNA control. The control DNA was processed as similar to the test sample for Bisulfite conversion and RCA. The RCA product proceeded for NGS.

4.9. RCA

RCA was performed in vitro using *ϕ29 DNA polymerase* which can amplify the bisulfite converted viral DNA. The reaction mix contained 1× *ϕ29 DNA polymerase* reaction Buffer, 1 mM dNTP mix, 50 µM Exo-resistant random primers and 50 ng of template DNA. The mixture was mixed gently and the total volume was made to 20 µL with nuclease free water. The template was denatured at 95 °C for 3 min and then cooled to room temperature. As soon as the mixture cooled, 5 units of *ϕ29 DNA polymerase* (Thermo Scientific, Waltham, MA, USA) and 0.02 units of *pyrophosphatase* (Thermo Scientific, Waltham, MA, USA) were added and incubated at 30 °C for 72 h. Finally, the enzyme was inactivated by incubating the reaction mix at 65 °C for 10 min. DNA amplification was confirmed on 0.8% agarose gel.

4.10. DNA Processing for Illumina Sequencing and Library Preparation

The RCA product was directly used as a template for Illumina sequencing to get the reads of bisulfite converted BYVMV viral DNA sequences [57]. For Illumina sequencing, 200 ng of DNA was sheared using Covaris S2 sonicator (Covaris, Woburn, MA, USA). This process generated 150 bp long DNA fragments and the fragment size distribution was checked on Agilent 2200 tape station with D1000 DNA screen tapes and reagents (Agilent Technologies, Santa Clara, CA, USA) and purified using high prep magnetic beads (Magbio Genomics, Gaithersburg, MD, USA). The purified fragments were end repaired, adenylated and ligated to Illumina multiplex barcode adapters, as per the kit protocol. Illumina Universal adapter (5′-AATGATACGGCGACCACCGAGATCTACACTCTTTCCCTACACGACGCTCTTCCGATCT-3′) and Index Adapter (5′-GATCGGAAGAGCACACGTCTGAACTCCAGTCAC [INDEX]ATCTCGTAT GCCGTCTTCTGCTTG-3′ [INDEX]) were used in this study. The adapter-ligated DNA was purified and amplified for 6 cycles of PCR using Illumina-compatible primers. The final PCR product was purified with high prep beads followed by primary quality control check. The Illumina-compatible sequencing library was initially quantified by Qubit fluorimeter (Thermo Scientific, Waltham, MA, USA) and its fragment distribution was analysed on Agilent 2200 Tape station.

4.11. Mapping Cytosine Methylation Using MethGo

MethGo is Python-based software designed for the analysis of data from whole genome bisulfite sequencing (WGBS) and reduced representation of bisulfite sequencing (RRBS) [28]. Prior to MethGo analysis, the WGBS reads should be proceeded for the removal of adapter sequences using trimmomatic software and aligned to the reference genome using BS-Seeker2. BS-Seeker2 performs genome editing, mapping bisulfite sequence reads against the given reference genome and calling methylation levels expeditiously [58]. We used MethGo and BS-Seeker2 for the analysis of DNA methylation by following the default settings. Coverage of methylation sites is a criterion for assessing the quality of methylation data. The COV module of MethGo software extracts the coverage for each cytosine from the BS-Seeker alignment file and generates a reverse cumulative plot for methylation sites in CG, CHG and CHH context (where H refers to A, C or T). The quality of NGS data can be easily evaluated by analysing the percentage of methylation sites covered and the depth of coverage (x). Methylation sites with high coverage is likely to provide accurate methylation status. The y-axis of the coverage map represents the percentage of methylation sites covered in the given genome from 0 to 100 and the x-axis represents the depth of coverage (x). The raw data resulting from BYVMV bisulfite NGS was deposited in NCBI Sequence Read Archive (SRA) with Bioproject reference number: PRJNA428793 (SRP128162).

Supplementary Materials: The following are available online at http://www.mdpi.com/2075-4655/2/2/7/s1.

Author Contributions: G.P., K.S.D.B. and A.G. conceived and designed experiments. K.S.D.B., A.G., J.K., K.K., P.S., S.A.C. and J.T. performed experiments. Data analysis was done by K.S.D.B., N.S., A.G. and G.P. Paper written by K.S.D.B., G.P., A.D.B. and A.G.

Acknowledgments: We thank Department of Science and Technology (DST), Government of India, New Delhi for giving INSPIRE fellowship to K.S.D.B. (Ref No: IF110735). Support from DBT (Ref: No. BT/PR2061/AGR/36/707/2011

dated 25-06-2013), SERB (Ref: No. SB/EMEQ-070/2013 dated 05-07-2013), DST-PURSE and UGC-SAP is greatly appreciated for the equipment grant. We express our gratitude to K. Veluthambi, and Sridevi from the School of Biotechnology, Madurai Kamaraj University for their valuable suggestions and lab facilities.

Conflicts of Interest: The authors declare no conflict of interest.

References

1. Varsani, A.; Roumagnac, P.; Fuchs, M.; Navas-Castillo, J.; Moriones, E.; Idris, A.; Briddon, R.W.; Rivera-Bustamante, R.; Murilo Zerbini, F.; Martin, D.P. Capulavirus and Grablovirus: Two new genera in the family Geminiviridae. *Arch. Virol.* **2017**, *162*, 1819–1831. [CrossRef] [PubMed]
2. Brown, J.K.; Zerbini, F.M.; Navas-Castillo, J.; Moriones, E.; Ramos-Sobrinho, R.; Silva, J.C.F.; Fiallo-Olivé, E.; Briddon, R.W.; Hernández-Zepeda, C.; Idris, A.; et al. Revision of Begomovirus taxonomy based on pairwise sequence comparisons. *Arch. Virol.* **2015**, *160*, 1593–1619. [CrossRef] [PubMed]
3. Hanley-Bowdoin, L.; Bejarano, E.R.; Robertson, D.; Mansoor, S. Geminiviruses: Masters at redirecting and reprogramming plant processes. *Nat. Rev. Microbiol.* **2013**, *11*, 777–788. [CrossRef] [PubMed]
4. Schneider, R.J.; Mohr, I. Translation initiation and viral tricks. *Trends Biochem. Sci.* **2003**, *28*, 130–136. [CrossRef]
5. Pilartz, M.; Jeske, H. Mapping of abutilon mosaic geminivirus minichromosomes. *J. Virol.* **2003**, *77*, 10808–10818. [CrossRef] [PubMed]
6. Velayudha Vimala Kumar, K.; Srikakulam, N.; Padbhanabhan, P.; Pandi, G. Deciphering microRNAs and Their Associated Hairpin Precursors in a Non-Model Plant, Abelmoschus esculentus. *Non Coding RNA* **2017**, *3*, 19. [CrossRef] [PubMed]
7. Raja, P.; Sanville, B.C.; Buchmann, R.C.; Bisaro, D.M. Viral Genome Methylation as an Epigenetic Defense against Geminiviruses. *J. Virol.* **2008**, *82*, 8997–9007. [CrossRef] [PubMed]
8. Ermak, G.; Paszkowski, U.; Wohlmuth, M.; Scheid, O.M.; Paszkowski, J. Cytosine methylation inhibits replication of African cassava mosaic virus by two distinct mechanisms. *Nucleic Acids Res.* **1993**, *21*, 3445–3450. [CrossRef] [PubMed]
9. Raja, P.; Wolf, J.N.; Bisaro, D.M. RNA silencing directed against geminiviruses: Post-transcriptional and epigenetic components. *Biochim. Biophys. Acta BBA Gene Regul. Mech.* **2010**, *1799*, 337–351. [CrossRef] [PubMed]
10. Ashapkin, V.V.; Kutueva, L.I.; Vanyushin, B.F. Plant DNA Methyltransferase Genes: Multiplicity, Expression, Methylation Patterns. *Biochem. Biokhimiia* **2016**, *81*, 141–151. [CrossRef] [PubMed]
11. Mitsudome, T.; Mon, H.; Xu, J.; Li, Z.; Lee, J.M.; Patil, A.A.; Masuda, A.; Iiyama, K.; Morokuma, D.; Kusakabe, T. Biochemical characterization of maintenance DNA methyltransferase DNMT-1 from silkworm, Bombyx mori. *Insect Biochem. Mol. Biol.* **2015**, *58*, 55–65. [CrossRef] [PubMed]
12. Pavlopoulou, A.; Kossida, S. Plant cytosine-5 DNA methyltransferases: Structure, function, and molecular evolution. *Genomics* **2007**, *90*, 530–541. [CrossRef] [PubMed]
13. Hashimshony, T.; Zhang, J.; Keshet, I.; Bustin, M.; Cedar, H. The role of DNA methylation in setting up chromatin structure during development. *Nat. Genet.* **2003**, *34*, 187–192. [CrossRef] [PubMed]
14. Severin, P.M.D.; Zou, X.; Gaub, H.E.; Schulten, K. Cytosine methylation alters DNA mechanical properties. *Nucleic Acids Res.* **2011**, *39*, 8740–8751. [CrossRef] [PubMed]
15. Bisaro, D.M. Silencing suppression by geminivirus proteins. *Virology* **2006**, *344*, 158–168. [CrossRef] [PubMed]
16. Rodríguez-Negrete, E.; Lozano-Durán, R.; Piedra-Aguilera, A.; Cruzado, L.; Bejarano, E.R.; Castillo, A.G. Geminivirus Rep protein interferes with the plant DNA methylation machinery and suppresses transcriptional gene silencing. *New Phytol.* **2013**, *199*, 464–475. [CrossRef] [PubMed]
17. Wang, B.; Li, F.; Huang, C.; Yang, X.; Qian, Y.; Xie, Y.; Zhou, X. V2 of tomato yellow leaf curl virus can suppress methylation-mediated transcriptional gene silencing in plants. *J. Gen. Virol.* **2014**, *95*, 225–230. [CrossRef] [PubMed]
18. Yang, X.; Xie, Y.; Raja, P.; Li, S.; Wolf, J.N.; Shen, Q.; Bisaro, D.M.; Zhou, X. Suppression of methylation-mediated transcriptional gene silencing by βC1-SAHH protein interaction during geminivirus-β satellite infection. *PLoS Pathog.* **2011**, *7*, e1002329. [CrossRef] [PubMed]
19. Jose, J.; Usha, R. Bhendi yellow vein mosaic disease in India is caused by association of a DNA β satellite with a begomovirus. *Virology* **2003**, *305*, 310–317. [CrossRef] [PubMed]

20. Priyavathi, P.; Kavitha, V.; Gopal, P. Complex Nature of Infection Associated with Yellow Vein Mosaic Disease in Bhendi (*Abelmoschus esculentus*). *Curr. Sci.* **2016**, *111*, 1511–1515. [CrossRef]
21. Chandran, S.A.; Levy, Y.; Mett, A.; Belausov, E.; Ramakrishnan, U.; Gafni, Y. Mapping of functional region conferring nuclear localization and karyopherin α-binding activity of the C2 protein of bhendi yellow vein mosaic virus. *J. Gen. Virol.* **2012**, *93*, 1367–1374. [CrossRef] [PubMed]
22. Gopal, P.; Pravin Kumar, P.; Sinilal, B.; Jose, J.; Kasin Yadunandam, A.; Usha, R. Differential roles of C4 and βC1 in mediating suppression of post-transcriptional gene silencing: Evidence for transactivation by the C2 of Bhendi yellow vein mosaic virus, a monopartite begomovirus. *Virus Res.* **2007**, *123*, 9–18. [CrossRef] [PubMed]
23. Chandran, S.A.; Jeyabharathy, C.; Usha, R. The C2 protein of Bhendi yellow vein mosaic virus plays an important role in symptom determination and virus replication. *Virus Genes* **2014**, *48*, 203–207. [CrossRef] [PubMed]
24. Rigden, J.E.; Krake, L.R.; Rezaian, M.A.; Dry, I.B. ORF C4 of tomato leaf curl geminivirus is a determinant of symptom severity. *Virology* **1994**, *204*, 847–850. [CrossRef] [PubMed]
25. Shen, Q.; Liu, Z.; Song, F.; Xie, Q.; Hanley-Bowdoin, L.; Zhou, X. Tomato SlSnRK1 protein interacts with and phosphorylates βC1, a pathogenesis protein encoded by a geminivirus β-satellite. *Plant Physiol.* **2011**, *157*, 1394–1406. [CrossRef] [PubMed]
26. Saeed, M.; Behjatnia, S.A.A.; Mansoor, S.; Zafar, Y.; Hasnain, S.; Rezaian, M.A. A single complementary-sense transcript of a geminiviral DNA β satellite is determinant of pathogenicity. *Mol. Plant Microbe Interact. MPMI* **2005**, *18*, 7–14. [CrossRef] [PubMed]
27. Yang, J.-Y.; Iwasaki, M.; Machida, C.; Machida, Y.; Zhou, X.; Chua, N.-H. βC1, the pathogenicity factor of TYLCCNV, interacts with AS1 to alter leaf development and suppress selective jasmonic acid responses. *Genes Dev.* **2008**, *22*, 2564–2577. [CrossRef] [PubMed]
28. Liao, W.-W.; Yen, M.-R.; Ju, E.; Hsu, F.-M.; Lam, L.; Chen, P.-Y. MethGo: A comprehensive tool for analyzing whole-genome bisulfite sequencing data. *BMC Genom.* **2015**, *16* (Suppl. 12), S11. [CrossRef] [PubMed]
29. Xie, Y.; Zhao, L.; Jiao, X.; Jiang, T.; Gong, H.; Wang, B.; Briddon, R.W.; Zhou, X. A recombinant begomovirus resulting from exchange of the C4 gene. *J. Gen. Virol.* **2013**, *94*, 1896–1907. [CrossRef] [PubMed]
30. Vanitharani, R.; Chellappan, P.; Pita, J.S.; Fauquet, C.M. Differential roles of AC2 and AC4 of cassava geminiviruses in mediating synergism and suppression of posttranscriptional gene silencing. *J. Virol.* **2004**, *78*, 9487–9498. [CrossRef] [PubMed]
31. Llave, C.; Kasschau, K.D.; Carrington, J.C. Virus-encoded suppressor of posttranscriptional gene silencing targets a maintenance step in the silencing pathway. *Proc. Natl. Acad. Sci. USA* **2000**, *97*, 13401–13406. [CrossRef] [PubMed]
32. Vanitharani, R.; Chellappan, P.; Fauquet, C.M. Geminiviruses and RNA silencing. *Trends Plant Sci.* **2005**, *10*, 144–151. [CrossRef] [PubMed]
33. Wang, X.-B.; Wu, Q.; Ito, T.; Cillo, F.; Li, W.-X.; Chen, X.; Yu, J.-L.; Ding, S.-W. RNAi-mediated viral immunity requires amplification of virus-derived siRNAs in Arabidopsis thaliana. *Proc. Natl. Acad. Sci. USA* **2010**, *107*, 484–489. [CrossRef] [PubMed]
34. Wang, H.; Hao, L.; Shung, C.-Y.; Sunter, G.; Bisaro, D.M. Adenosine Kinase Is Inactivated by Geminivirus AL2 and L2 Proteins. *Plant Cell* **2003**, *15*, 3020–3032. [CrossRef] [PubMed]
35. Zhang, Z.; Chen, H.; Huang, X.; Xia, R.; Zhao, Q.; Lai, J.; Teng, K.; Li, Y.; Liang, L.; Du, Q.; et al. BSCTV C2 Attenuates the Degradation of SAMDC1 to Suppress DNA Methylation-Mediated Gene Silencing in *Arabidopsis*. *Plant Cell Online* **2011**, *23*, 273–288. [CrossRef] [PubMed]
36. Cui, X.; Zhou, X. AC2 and AC4 proteins of Tomato yellow leaf curl China virus and Tobacco curly shoot virus mediate suppression of RNA silencing. *Chin. Sci. Bull.* **2004**, *49*, 2607–2612. [CrossRef]
37. Stanley, J.; Latham, J.R.; Pinner, M.S.; Bedford, I.; Markham, P.G. Mutational analysis of the monopartite geminivirus beet curly top virus. *Virology* **1992**, *191*, 396–405. [CrossRef]
38. Jupin, I.; De Kouchkovsky, F.; Jouanneau, F.; Gronenborn, B. Movement of tomato yellow leaf curl geminivirus (TYLCV): Involvement of the protein encoded by ORF C4. *Virology* **1994**, *204*, 82–90. [CrossRef] [PubMed]
39. Krake, L.R.; Rezaian, M.A.; Dry, I.B. Expression of the Tomato Leaf Curl Geminivirus C4 Gene Produces Viruslike Symptoms in Transgenic Plants. *Mol. Plant. Microbe Interact.* **1998**, *11*, 413–417. [CrossRef]

40. Latham, J.R.; Saunders, K.; Pinner, M.S.; Stanley, J. Induction of plant cell division by beet curly top virus gene C4. *Plant J.* **1997**, *11*, 1273–1283. [CrossRef]
41. Krichevsky, A.; Kozlovsky, S.V.; Gafni, Y.; Citovsky, V. Nuclear import and export of plant virus proteins and genomes. *Mol. Plant Pathol.* **2006**, *7*, 131–146. [CrossRef] [PubMed]
42. Kunik, T.; Palanichelvam, K.; Czosnek, H.; Citovsky, V.; Gafni, Y. Nuclear import of the capsid protein of tomato yellow leaf curl virus (TYLCV) in plant and insect cells. *Plant J. Cell Mol. Biol.* **1998**, *13*, 393–399. [CrossRef]
43. Palanichelvam, K.; Kunik, T.; Citovsky, V.; Gafni, Y. The capsid protein of tomato yellow leaf curl virus binds cooperatively to single-stranded DNA. *J. Gen. Virol.* **1998**, *79 Pt 11*, 2829–2833. [CrossRef] [PubMed]
44. Usha, R.; Zrachya, A.; Levy, Y.; Spanov, H.; Gafni, Y. Protein–protein interactions and nuclear trafficking of coat protein and βC1 protein associated with Bhendi yellow vein mosaic disease. *Virus Res.* **2006**, *122*, 127–136. [CrossRef]
45. Guha, D.; Poornima Priyadarshini, C.G.; Purakayastha, A.; Thippeswamy, R.; Lakshmikanth, M.; Savithri, H.S. Biochemical characterization of C4 protein of Cotton leaf curl Kokhran Virus-Dabawali. *Biochim. Biophys. Acta* **2013**, *1830*, 3734–3744. [CrossRef] [PubMed]
46. Rojas, M.R.; Jiang, H.; Salati, R.; Xoconostle-Cázares, B.; Sudarshana, M.R.; Lucas, W.J.; Gilbertson, R.L. Functional analysis of proteins involved in movement of the monopartite begomovirus, Tomato yellow leaf curl virus. *Virology* **2001**, *291*, 110–125. [CrossRef] [PubMed]
47. Buchmann, R.C.; Asad, S.; Wolf, J.N.; Mohannath, G.; Bisaro, D.M. Geminivirus AL2 and L2 proteins suppress transcriptional gene silencing and cause genome-wide reductions in cytosine methylation. *J. Virol.* **2009**, *83*, 5005–5013. [CrossRef] [PubMed]
48. Wang, H.; Buckley, K.J.; Yang, X.; Buchmann, R.C.; Bisaro, D.M. Adenosine kinase inhibition and suppression of RNA silencing by geminivirus AL2 and L2 proteins. *J. Virol.* **2005**, *79*, 7410–7418. [CrossRef] [PubMed]
49. Li, F.; Huang, C.; Li, Z.; Zhou, X. Suppression of RNA Silencing by a Plant DNA Virus Satellite Requires a Host Calmodulin-Like Protein to Repress RDR6 Expression. *PLoS Pathog.* **2014**, *10*, e1003921. [CrossRef] [PubMed]
50. Vieira, J.; Messing, J. New pUC-derived cloning vectors with different selectable markers and DNA replication origins. *Gene* **1991**, *100*, 189–194. [PubMed]
51. Ditta, G.; Stanfield, S.; Corbin, D.; Helinski, D.R. Broad host range DNA cloning system for gram-negative bacteria: Construction of a gene bank of Rhizobium meliloti. *Proc. Natl. Acad. Sci. USA* **1980**, *77*, 7347–7351. [CrossRef] [PubMed]
52. Jose, J.; Usha, R. Extraction of geminiviral DNA from a highly mucilaginous plant (*Abelmoschus esculentus*). *Plant Mol. Biol. Rep.* **2000**, *18*, 349–355. [CrossRef]
53. Hong, Y. Virus Resistance in *Nicotiana benthamiana* Conferred by African Cassava Mosaic Virus Replication-Associated Protein (ACI) Transgene. *Mol. Plant. Microbe Interact.* **1996**, *9*, 219–255. [CrossRef]
54. Karthikeyan, C.; Patil, B.L.; Borah, B.K.; Resmi, T.R.; Turco, S.; Pooggin, M.M.; Hohn, T.; Veluthambi, K. Emergence of a Latent Indian Cassava Mosaic Virus from Cassava Which Recovered from Infection by a Non-Persistent Sri Lankan Cassava Mosaic Virus. *Viruses* **2016**, *8*, 264. [CrossRef] [PubMed]
55. Yoo, S.-D.; Cho, Y.-H.; Sheen, J. Arabidopsis mesophyll protoplasts: A versatile cell system for transient gene expression analysis. *Nat. Protoc.* **2007**, *2*, 1565–1572. [CrossRef] [PubMed]
56. Paprotka, T.; Deuschle, K.; Metzler, V.; Jeske, H. Conformation-Selective Methylation of Geminivirus DNA. *J. Virol.* **2011**, *85*, 12001–12012. [CrossRef] [PubMed]
57. Deuschle, K.; Kepp, G.; Jeske, H. Differential methylation of the circular DNA in geminiviral minichromosomes. *Virology* **2016**, *499*, 243–258. [CrossRef] [PubMed]
58. Guo, W.; Fiziev, P.; Yan, W.; Cokus, S.; Sun, X.; Zhang, M.Q.; Chen, P.-Y.; Pellegrini, M. BS-Seeker2: A versatile aligning pipeline for bisulfite sequencing data. *BMC Genom.* **2013**, *14*, 774. [CrossRef] [PubMed]